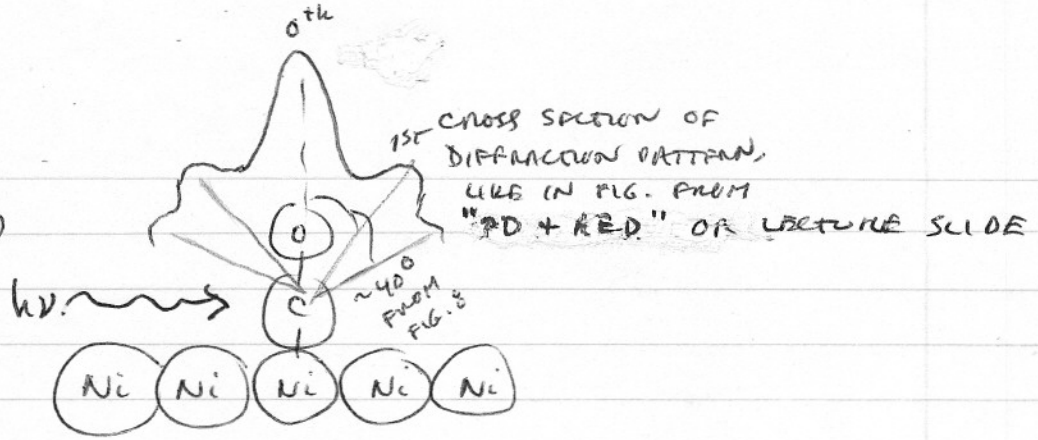
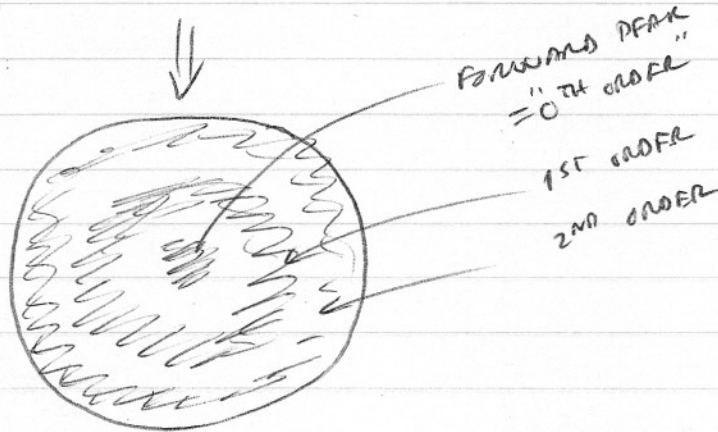


20 points

[4.5] (a)



SO 2D PLOT OF
 HEMISPHERE
 DATA IS
 LIKE:



(b) JUST USE $l_{max} = kr_{MUFFIN-TIN}$
 WITH:

$$E_{kin} \approx 1486.6 - 284 \approx 1202 \text{ eV}$$

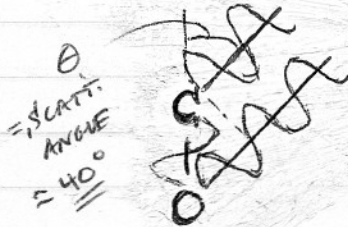
$$k = 0.512 (1202)^{1/2} = 17.8 \text{ \AA}^{-1}$$

SO

$$l_{max} = (17.8)(1.1) = 19.5 \Rightarrow \underline{\underline{20}}$$

(c) FOR FIRST-ORDER INTERFERENCE: $n=1$

$$2\pi = kr_{c-o} (1 - \cos \theta_1) + \psi_0(\theta_1)$$

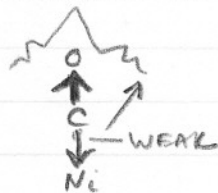


$$2\pi = 17.8 (1.10) (1 - \cos(40^\circ)) + \psi_0(\theta_1)$$

$$6.28 - 4.91 = \psi_0(\theta_1)$$

$$\psi_0(\theta_1) = \underline{\underline{1.37 \text{ rad}}} \approx \underline{\underline{78^\circ}}$$

(d) See following pages, with brief answers as:
1st order = 6th order, due to dominance of single
forward scattering like:



(e) See following pages as well, with brief answers as:
Lowering energy increases photoe⁻ wavelength and
makes rings larger in diameter
" " also increases importance of multiple
scattering, as well as Ni backscattering, but
single-scattering picture still an excellent
description.



Answers to parts (d) and (e):

Cluster definition

The cluster and the list of emitters are defined by a list of commands with the following format (click here or on the items of this list for further details):

atom symbol $x y z$ layer symbol $x y z a b \alpha_1 \alpha_2$
surface symbol $x y z a$ type emitter $x y z$

Fill in the text box with these commands according to the cluster specifications that you need. Some examples are provided by clicking here (you may cut and paste them to this page and modify them further).

```
atom O 0 0 1.18  
atom C 0 0 0  
atom Ni 0 0 -1.83  
emitter 0 0 0  
end
```

The cluster consists of a maximum of atoms. (Warning: a finite number of atoms generally introduces symmetry breaking.)

The size of the cluster is determined by the distance $d_{\max} =$ Å and the reference point $x_0 =$ Å,
 $y_0 =$ Å, $z_0 =$ Å.

See cluster shape for more details.

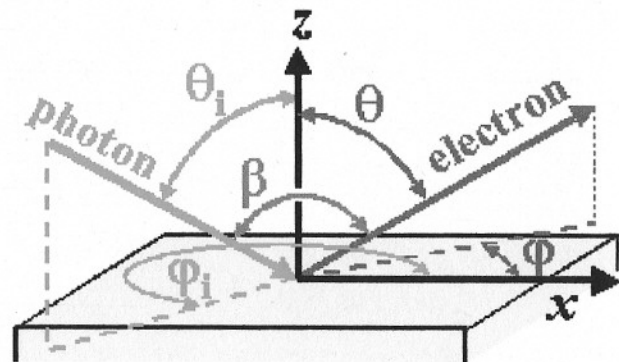
Geometry of beam and analyzer

Incoming beam parameters (see figure)

Polar angle $\theta_i =$ degrees

Azimuthal angle $\varphi_i =$ degrees

- Polarization:
- p-polarization
 - s-polarization
 - RCP
 - LCP



Schematic representation of the geometry

Mobility of cluster
beam, and sample
(click here for details):

- Only the sample moves with constant $\beta =$ degrees
- Only the analyzer moves
- Both the sample and the analyzer move

Could do it

this way too: see later

Note: the parameter β specifies the angle between beam and analyzer when this is kept constant during the simulation (i.e., everything happens as if it is only the sample that is rotated); therefore, this parameter is not required when only the analyzer moves or when both the sample and the analyzer move (click here for details).

Energy and angle scanning parameters (see figure above)

The following entries will select the range of photoelectron energies and angles of emission.

Energy scans for a given emission angle can be chosen by selecting more than one energy of emission and only one polar angle and one azimuthal angle (the value of each angle is then taken as the lower limit of the selected angular range, and the value of the upper limits are disregarded). In this case, the output is a 1D plot with the photoelectron intensity as a function of photoelectron energy.

Angular scans can be chosen by selecting only one photoelectron energy. Then, if the polar and the azimuthal angles take both more than one value, the output is a 2D polar plot of the photoelectron intensity. Otherwise, if only one polar angle is selected, a 1D plot is generated (an azimuthal scan), whereas if only one azimuthal angle is selected then a 1D polar plot is given in the output.

For 2D angular scans, a linear or logarithmic scale of the photoelectron intensities can be selected for the grey scale (see below). More details about the 2D representation (e.g., type of projection on 2D) are given in the caption of the output.

Electron energy range: equally-spaced value(s) of the electron energy from eV to eV

Polar angle: equally-spaced value(s) of the polar angle θ from degrees to degrees

Azimuthal angle: equally-spaced value(s) of the azimuthal angle ϕ from degrees to degrees

Type of 2D angular representation: Linear scale
 Logarithmic scale

Type of azimuthal of polar angular representation: Cartesian
 Polar

Use Ni
Nearest-neighbor
distance

Multiple scattering parameters

Internal code parameters

Maximum orbital quantum number $l_{\max} =$

Scattering order =

Iteration method:
 Jacobi (regular MS)
 Recursion + **6 for second part**

Additional solid parameters

Inner potential $V_0 =$ eV

Electronic edge $z_0 =$ Å

Inelastic mean free path: either choose a fixed value = Å

or (if that last entry is <0) use the TPP-2M formula for Ni

with parameters $\rho =$ g/cm³, $N_v =$, $E_p =$

eV, and $E_g =$ eV

Temperature (K) = and Debye temperature (K) =

Use band
structure
plus work
function

TPP-2M

Initial core-state quantum numbers

Radial matrix elements:
 Automatic: core level (e.g. 1s, 2s, 2p, etc.) =
 Manual: $l_0 =$, $R_{l_0+1} =$, $\delta_{l_0+1} =$, $R_{l_0-1} =$, $\delta_{l_0-1} =$

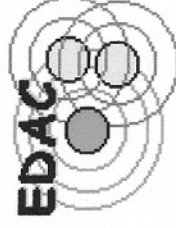
Calculate*

Download Input File**

Reset***

COMPUTATION TIME: the CPU time needed for the calculation using the default cluster and input parameters (use Reset to recover default input) is 1.24 seconds on a Pentium III @ 733 MHz. This gives a time scale to estimate the computation time for other input parameters, keeping in mind that it scales like $\sim (n_{\text{scat}} -$

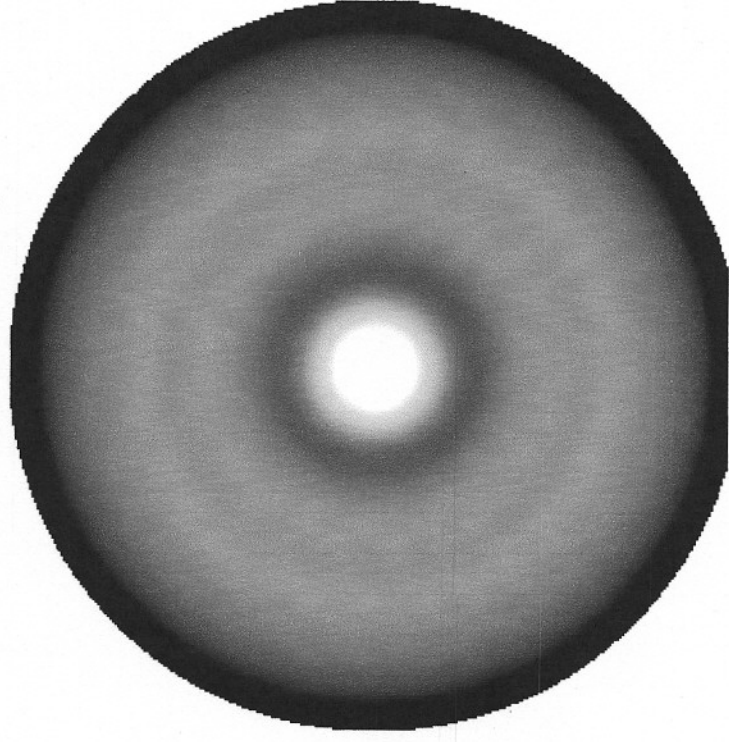
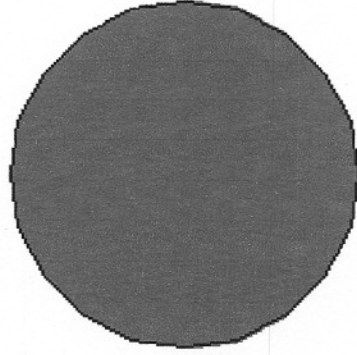
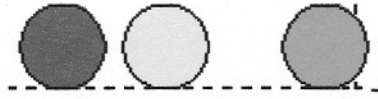
EDAC output for O-C-Ni



[Click on the figure to download data.](#)

1202 eV

1st order only

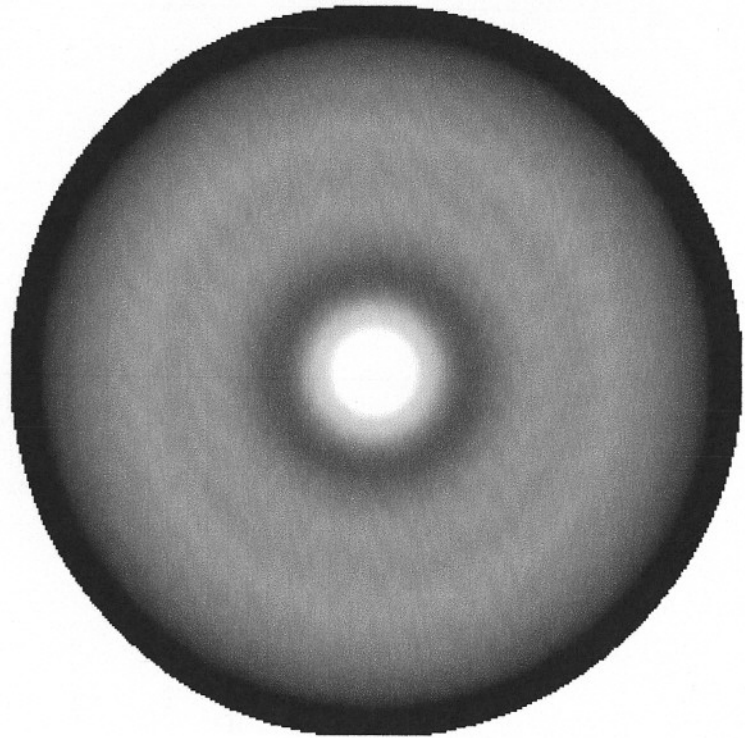
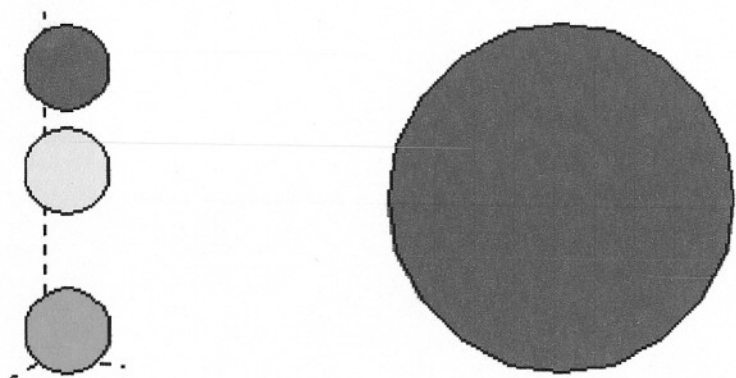


EDAC output for O-C-Ni



Click on the figure to download data.

1202 eV, 6th order—
no difference,
fwd. scatt. dominant



Alternate geometry setup, with analyzer moving only

Geometry of beam and analyzer

Incoming beam parameters (see figure)

Polar angle $\theta_i =$ degrees

Azimuthal angle $\varphi_i =$ degrees

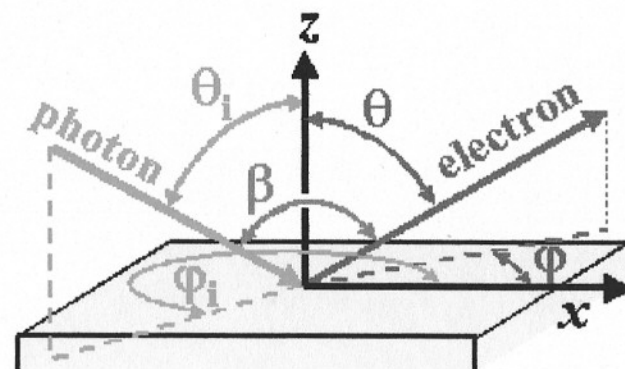
p-polarization

s-polarization

RCP

LCP

Polarization:



Schematic representation of the geometry

Mobility of cluster
beam, and sample

(click here for details):

Only the sample moves with constant $\beta =$ degrees

Only the analyzer moves

Both the sample and the analyzer move

Note: the parameter β specifies the angle between beam and analyzer when this is kept constant during the simulation (i.e., everything happens as if it is only the sample that is rotated); therefore, this parameter is not required when only the analyzer moves or when both the sample and the analyzer move (click here for details).

Alternate geometry setup, with analyzer moving only

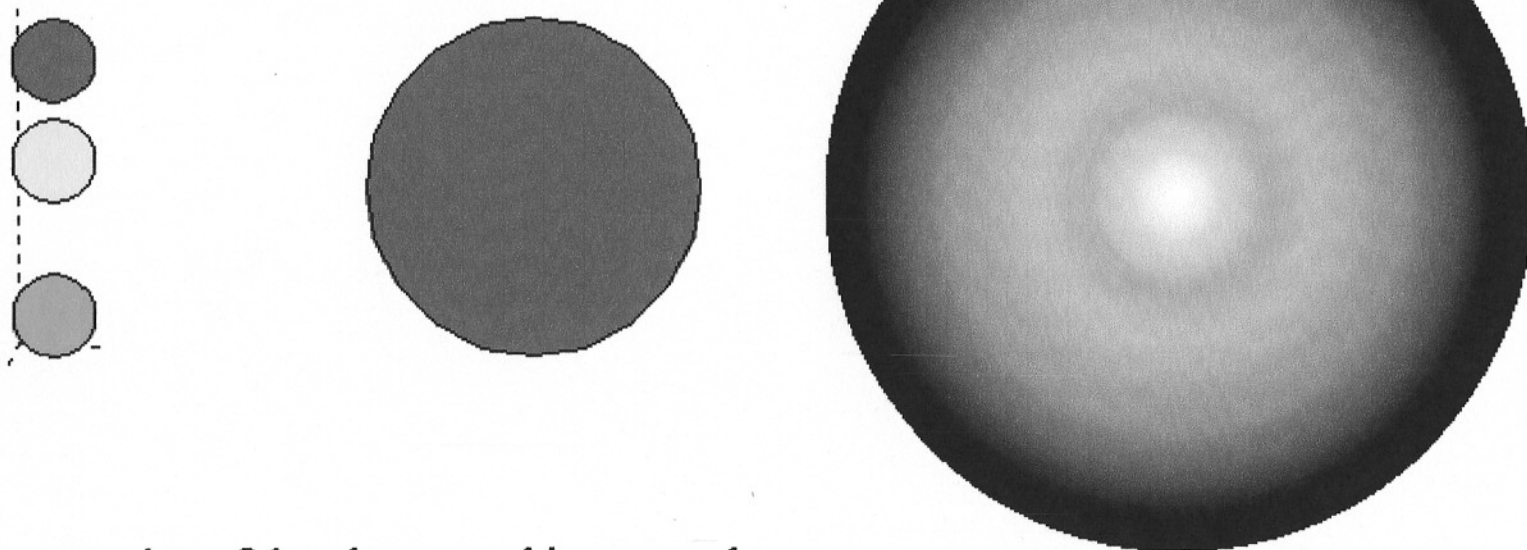
EDAC output for O-C-Ni



Click on the figure to download data.

1202 eV

6th order—rings more clear



Back to first geometry inputs, sample rotating

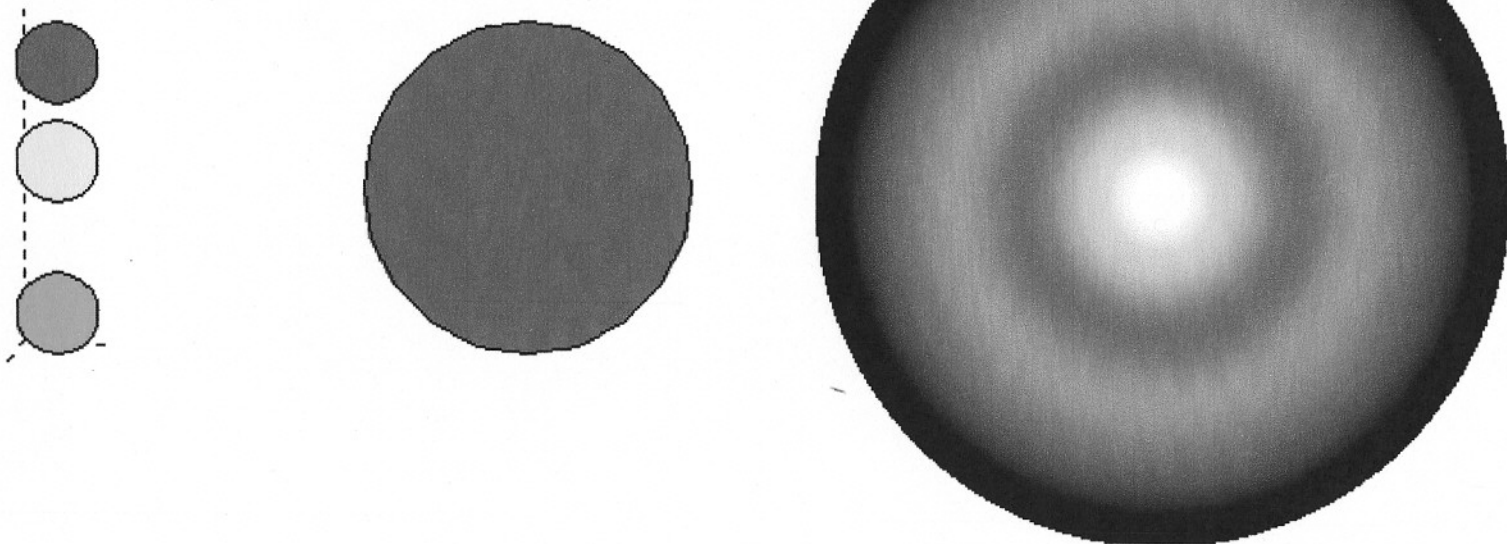
EDAC output for O-C-Ni



Click on the figure to download data.

100 eV

1st order



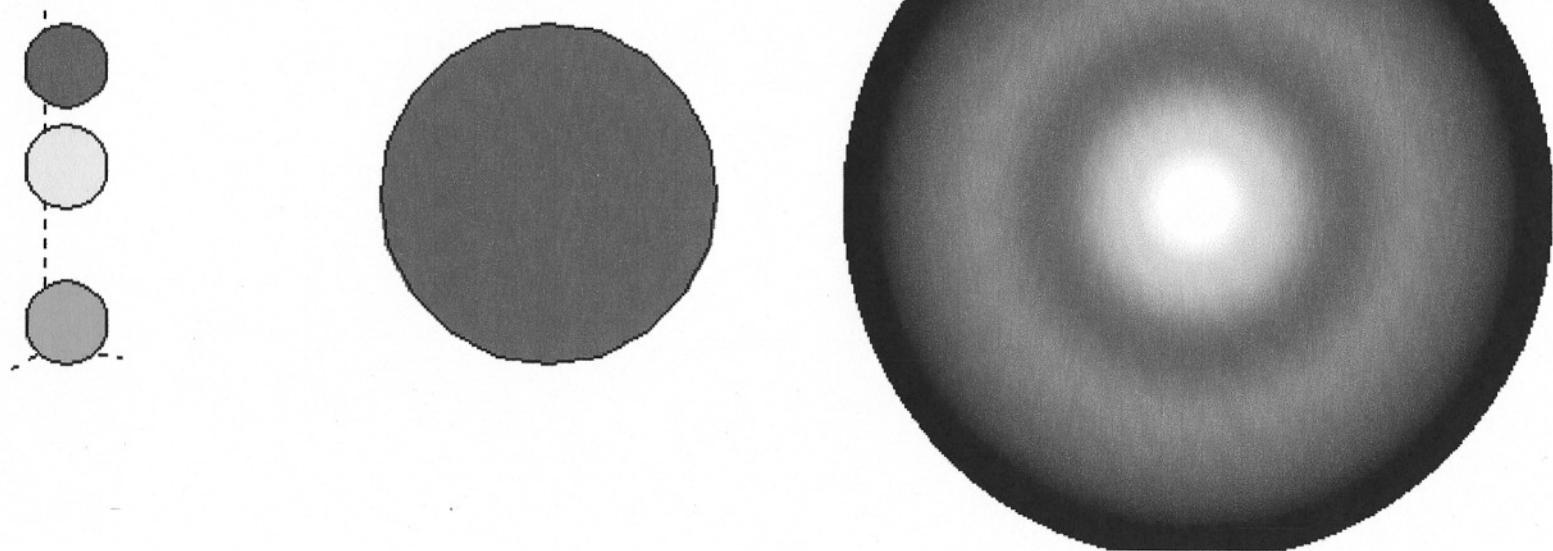
EDAC output for O-C-Ni



Click on the figure to download data.

100 eV

6th order—slight difference



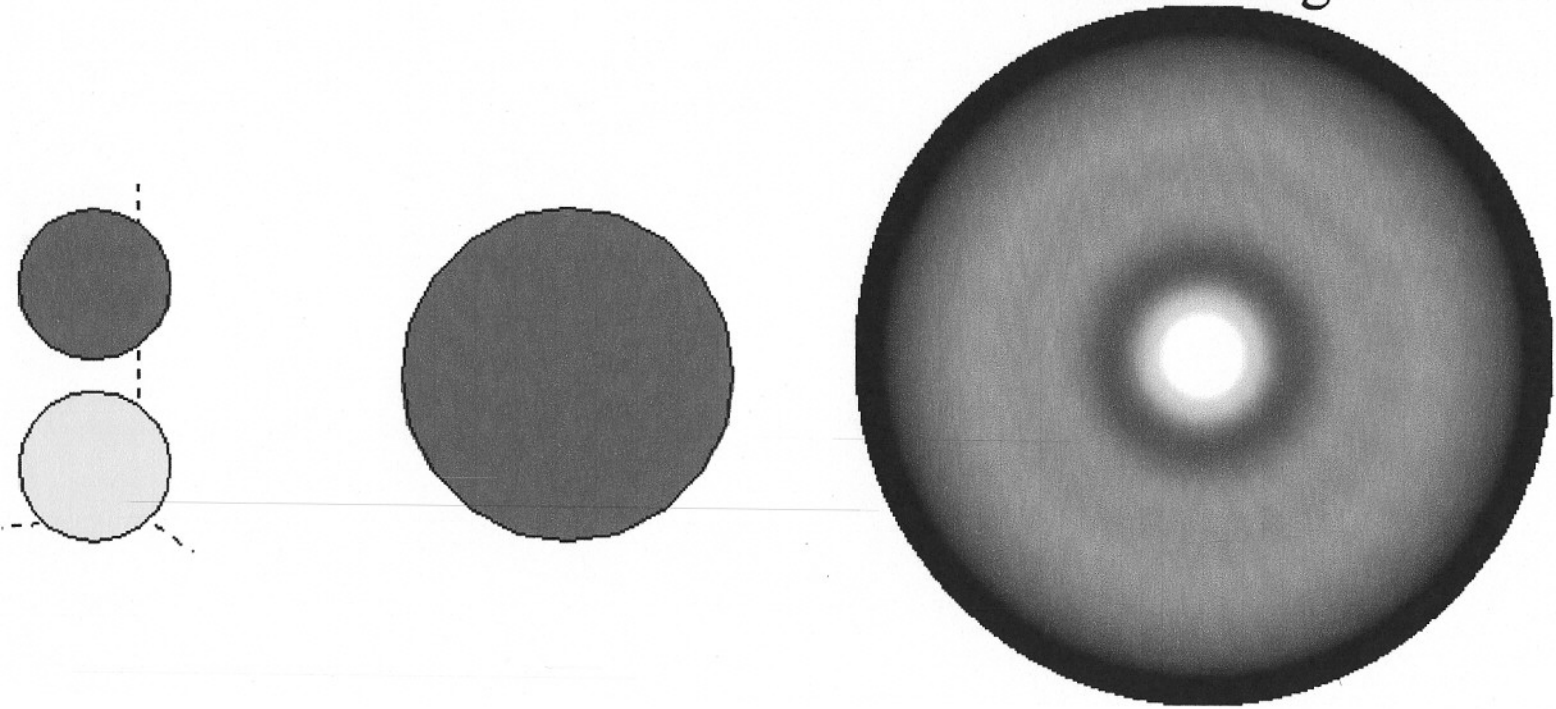
EDAC output for O-C-Ni



Click on the figure to download data.

1202 eV, no Ni

6th order—slight difference

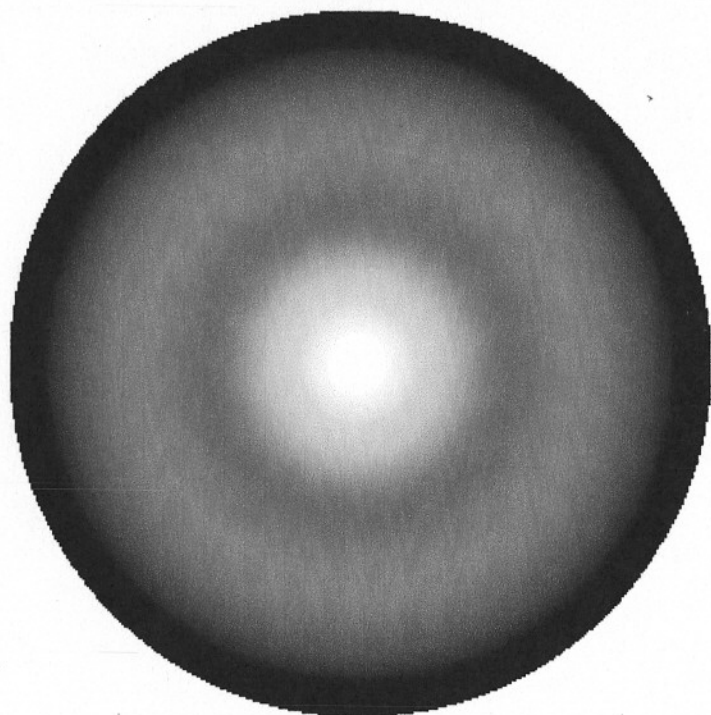
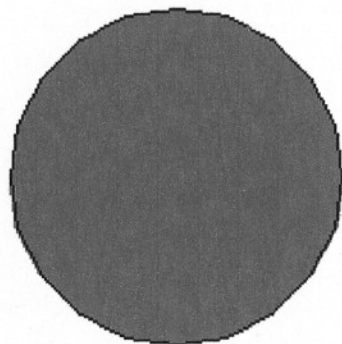
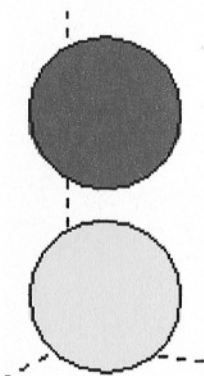


EDAC output for O-C-Ni



Click on the figure to download data. 100 eV, no Ni

6th order—slight difference



[4.7]

(a) The relevant equation is:

$$\sin\theta_{inc} + \sin\theta_{refl} = m\lambda_x/d$$

or

$$\sin\theta_{refl} = m\lambda_x/d - \sin\theta_{inc}$$

With fixed θ_{inc} , the derivative is calculated via:

$$d\sin\theta_{refl}/d\theta_{refl} = \cos\theta_{refl} = (m/d)d\lambda_x/d\theta_{refl}$$

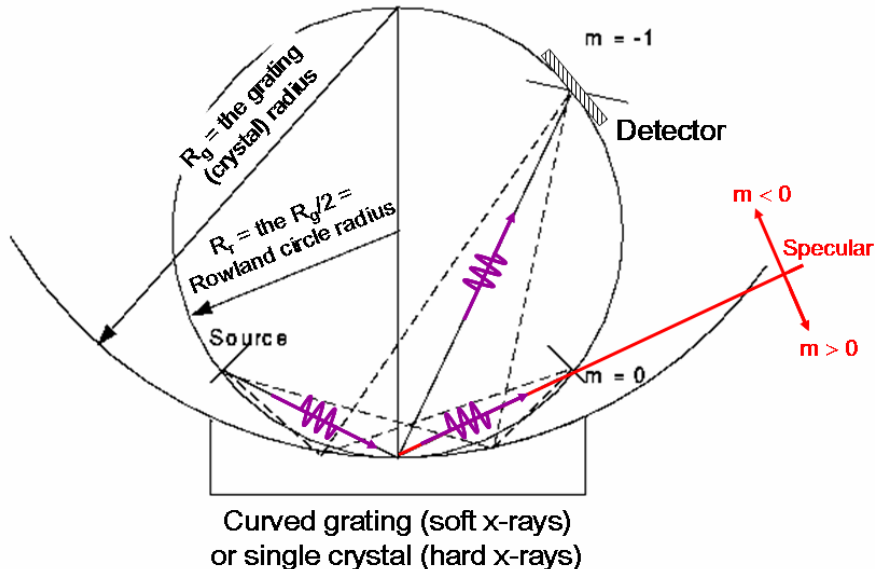
Thus,

$$d\theta_{refl}/d\lambda_x = m/(d\cos\theta_{refl}),$$

a quantity which is larger for higher order m , smaller line spacing d , or larger reflection angle θ_{refl} .

(b) The geometry is as introduced in lecture:

The (Focusing) Rowland Circle X-Ray Monochromator/Spectrometer Geometry



First use the grating equation to determine θ_{refl} ,

with parameters of $d = 1/1200$ mm = 8.33×10^{-4} mm = 8.33×10^{-7} m,

$\theta_{inc} = 1.9^\circ$, $\lambda_x = 12,398/500$ Å = 24.8 Å = 2.48×10^{-9} m, and assuming first-order reflection so $m = 1$, we have:

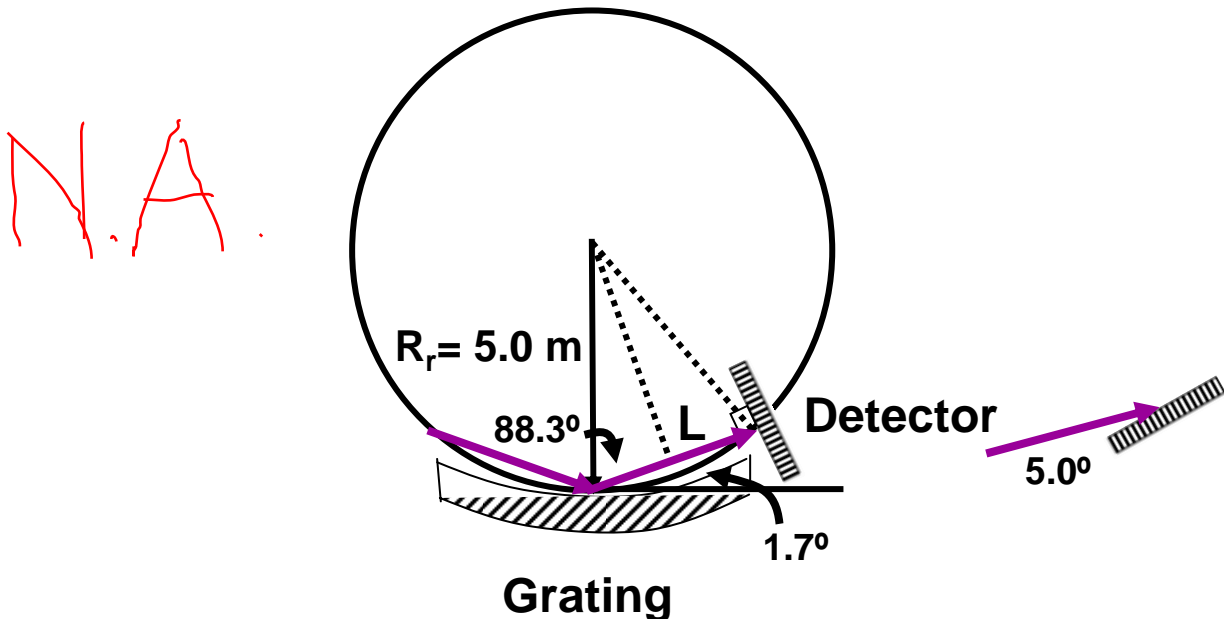
$$\sin\theta_{refl} = m\lambda_x/d - \sin\theta_{inc} = 1(2.48 \times 10^{-9})/8.33 \times 10^{-7} - \sin(1.9^\circ) = 0.0029 - 0.033 = -0.030, \text{ or } \theta_{refl} = 1.7^\circ. \text{ (cont'd)}$$

So this is nearly specular reflection, and the reflectivity is high for soft x-rays, another important consideration in the design.

Thus also,

$$d\theta_{refl}/d\lambda_x = m/(d\cos\theta_{refl}) = 1/(8.33 \times 10^{-7} \text{ m})\cos(1.7^\circ) \\ = 1.2 \times 10^6 \text{ radians/m} = 1.2 \times 10^3 \text{ radians/mm}$$

The change in wavelength for 0.1% energy resolution is from say 500 eV to 500.5 eV or from 24.796 Å to 24.771 Å and thus $\Delta\lambda_x = 0.025 \text{ Å} = 2.5 \times 10^{-9} \text{ mm}$, so $\Delta\theta_{refl} = (1.2 \times 10^3) \times (2.5 \times 10^{-9}) = 3.0 \times 10^{-6} \text{ radians}$



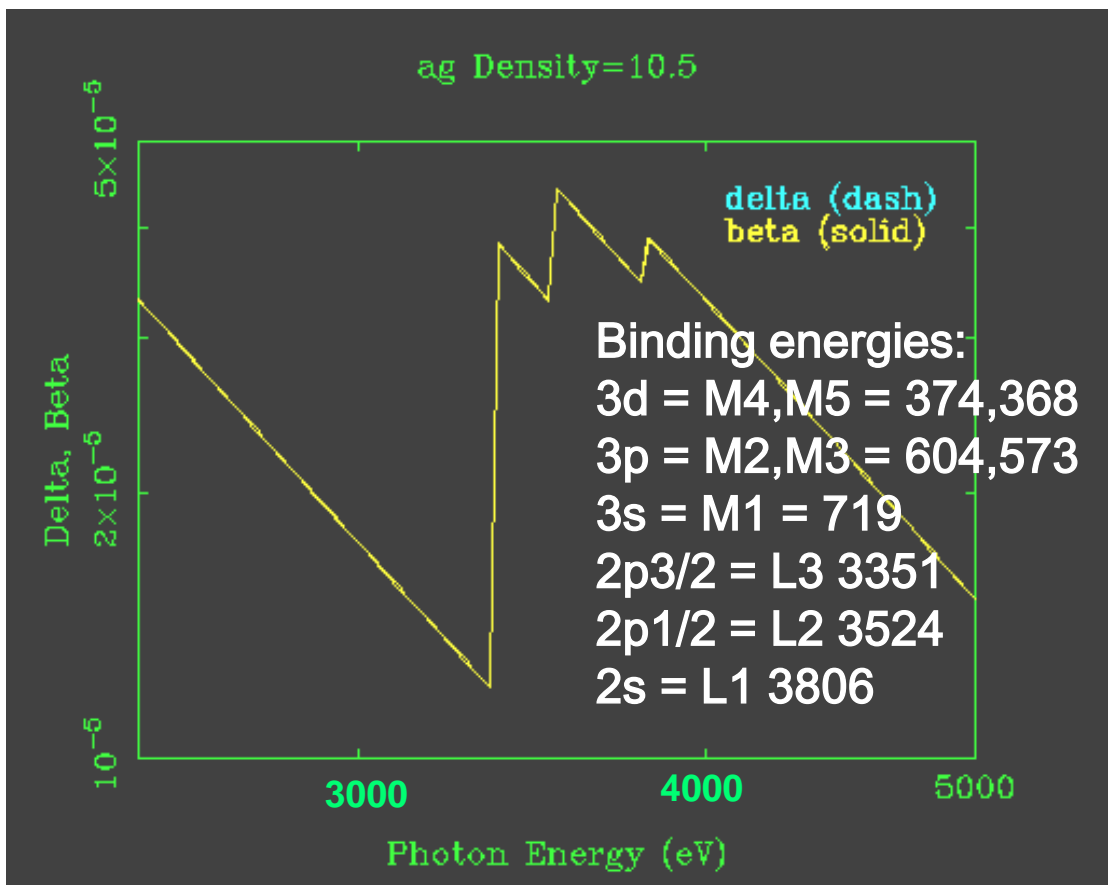
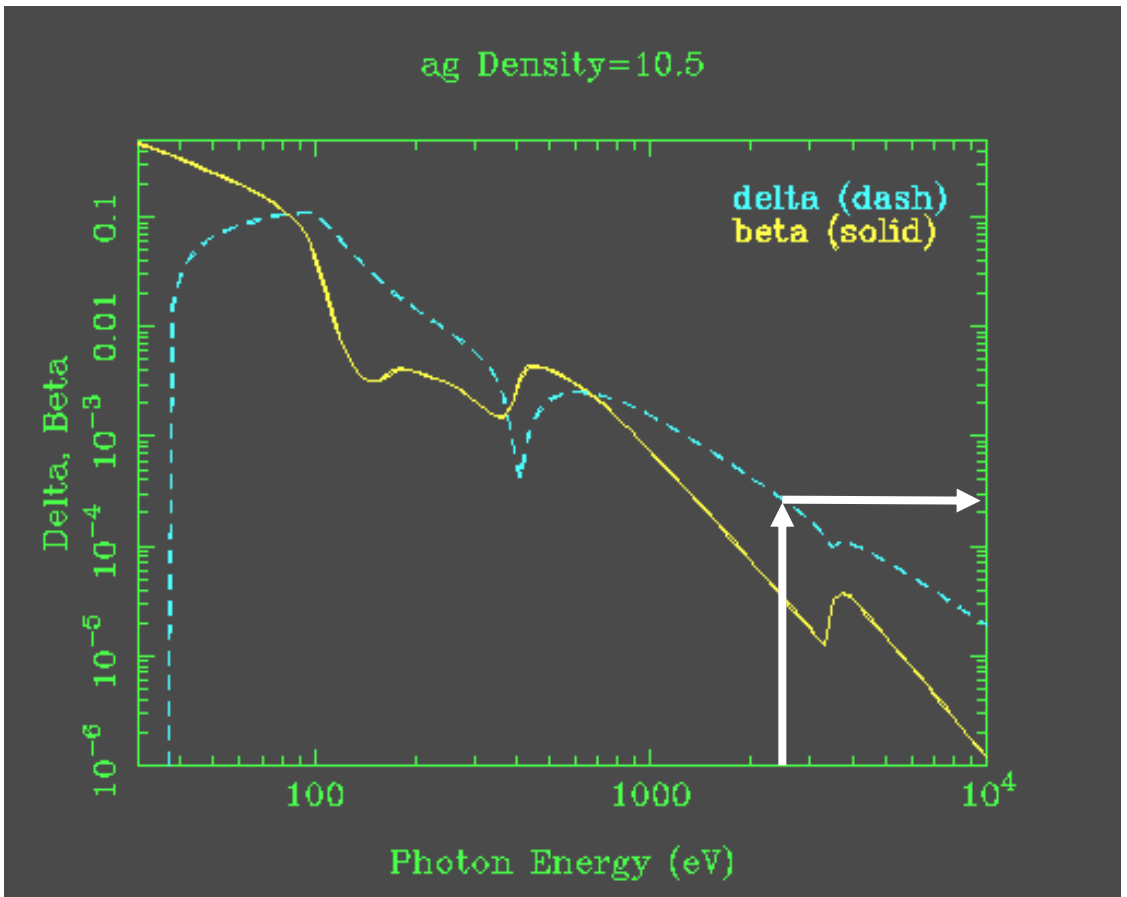
From the geometry above, the distance of the detector from the center of the grating is $L = 2R_r\cos(88.3^\circ) = 2(5.0\text{m})(0.029) = 0.296 \text{ m} = 296 \text{ mm}$.

Thus, the distance between two points separated by $\Delta\lambda_x$ at the detector will be $(3.0 \times 10^{-6})(296) = 8.88 \times 10^{-4} \text{ mm} = 8.88 \times 10^{-7} \text{ m} = 88.8 \text{ microns}$. So we would need resolution in the detector about $1/10^{\text{th}}$ of this or about 9 microns to adequately resolve this change in energy.

Reorienting the detector so that the light hits at a grazing incidence angle of 5° (see above left) simply increases the spacing of the detector channels as $1/(\sin\theta_{det}) = 11.5$, so we could relax the detector resolution to about 100 microns.

5.1 (a)

f



5.1 (a) (cont'd)

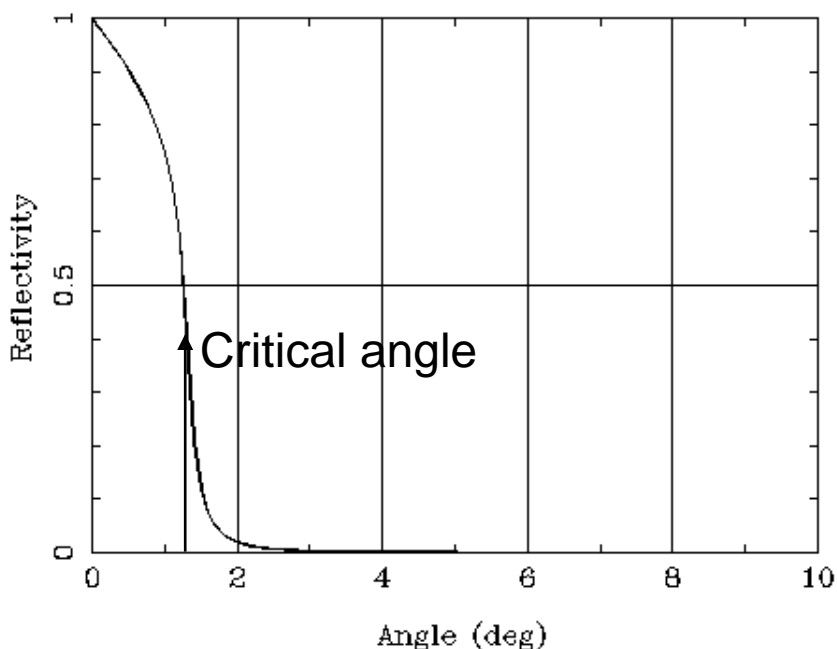
Yes, increases in beta over 2500-5000 eV are associated with turning on the absorption of the various levels in the $n = 2$ or L shell.

From binding energies for Ag L shell (see prior page), we see that three are needed, and three steps are seen in beta. Therefore, spin-orbit is included in this range of the tabulation of index of refraction.

(b) From the first plot on the prior page, the critical angle in this regime should be about $\sqrt{2\delta}^{1/2}$ in radians, or with $\delta \cong 2.5 \times 10^{-4}$ over the $n = 3$ absorption edges, this gives 0.223 radians or $0.0223(360/2\pi) = 0.0223(57.3 \text{ deg./radian}) = 1.3 \text{ deg}$. Plot below shows $R \cong 0.4$ at this angle.

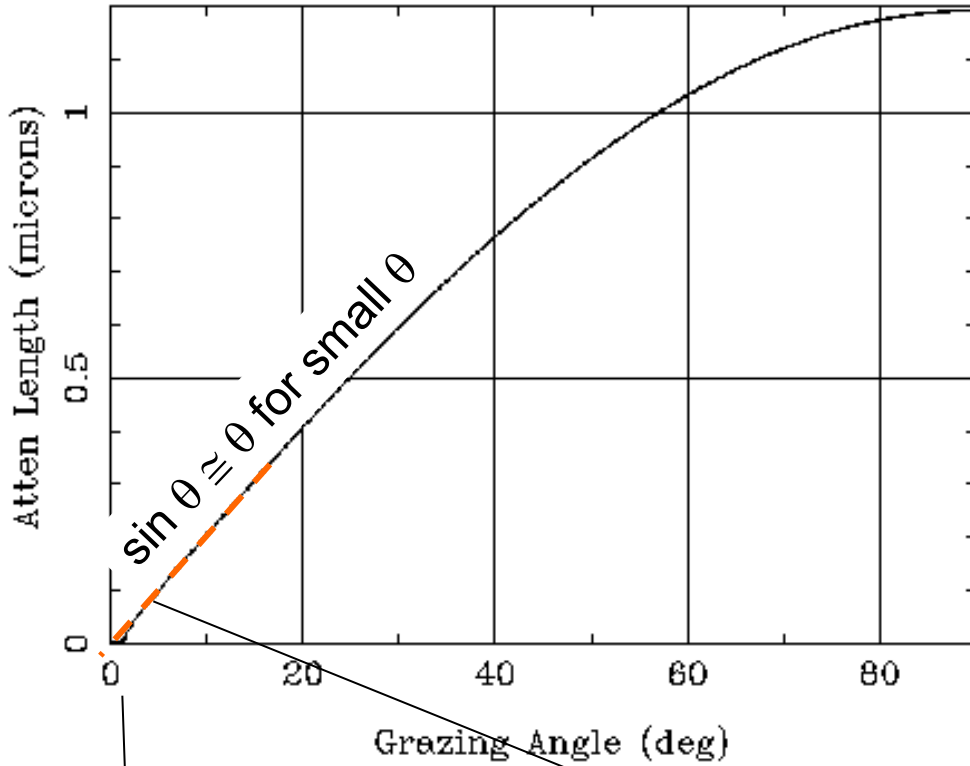
Mirror Reflectivity

ag Rho=10.5, Sig=0.nm, P=1., E=2500.eV

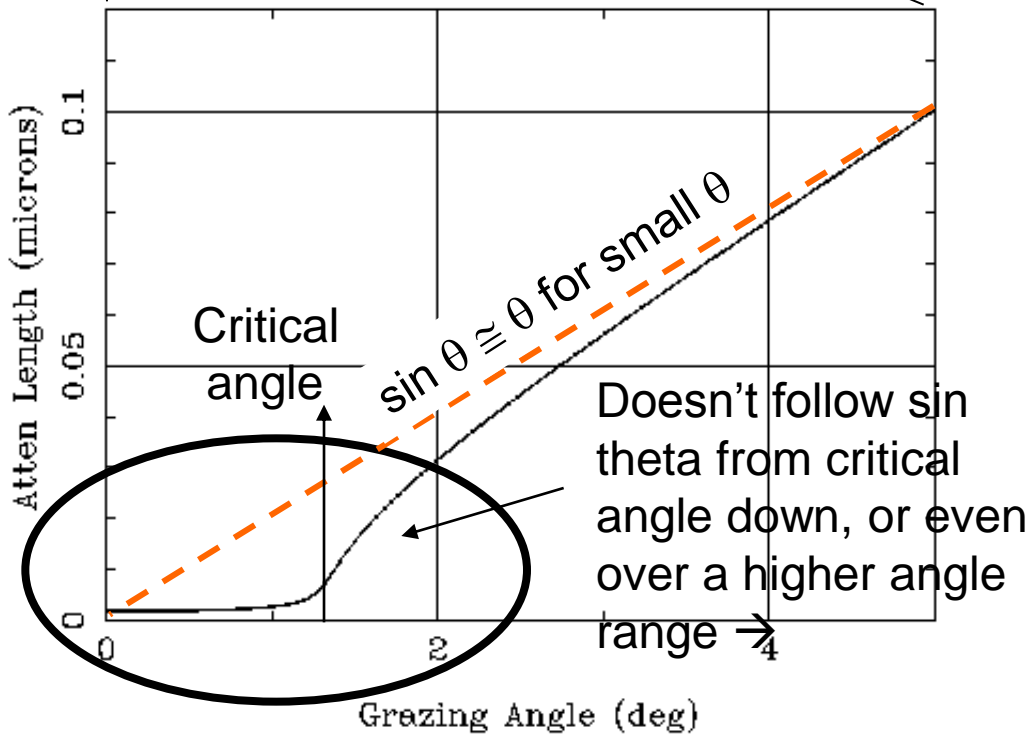


5.1 (c)

ag Density=10.5, Energy=2500.eV



ag Density=10.5, Energy=2500.eV



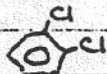
[5.2] (a) In each molecule, carbons at lower E_{kin} (higher E_b) are those bonded to Cl. Electronegative Cl withdraws valence charge, thereby increasing binding energy.

Relative intensities should to first order be proportional to no. of atoms, so

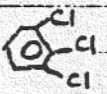
5

Molecule

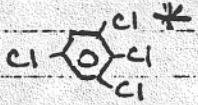
Predicted
Relative Intensity
C(Cl)/C(H)



$$2.0 / 4.0 = 0.5$$



$$3.0 / 3.0 = 1.0$$



$$4.0 / 2.0 = 2.0$$

These intensities are in good agreement with experiment, as can be verified by visual inspection.

* For this molecule, one might expect three kinds of carbon, three grouped C(Cl)'s, one isolated C(Cl), and 2 C(H)'s. However, nearest neighbor effects dominate the C(Cl) shift, so that all C(Cl)'s occur at the same E_b .

(b) This result is consistent with the potential model, which predicts that

$$E_b^V(\text{Cl}_s, \text{molecule}) = E_b^V(\text{Cl}_s, \text{free ion of charge } q_c) + \sum_{i \neq c} \frac{q_i}{r_{ci}}$$

5

or

$$E_b^V(\text{Cl}_s, \text{molecule}) - \sum_{i \neq c} \frac{q_i}{r_{ci}} = E_b^V(\text{Cl}_s, \text{free ion of charge } q_c),$$

provided that we make the identification

$$E_b^V(\text{Cl}_s, \text{free ion of charge } q_c) = 284.9 + 23.3 q_c.$$

The significance of the constants is thus:

$284.9 = E_b^V(\text{Cl}_s, \text{free atom}, q_c=0)$
$23.3 = q_c \approx J_{1s\text{-valence}}$

5

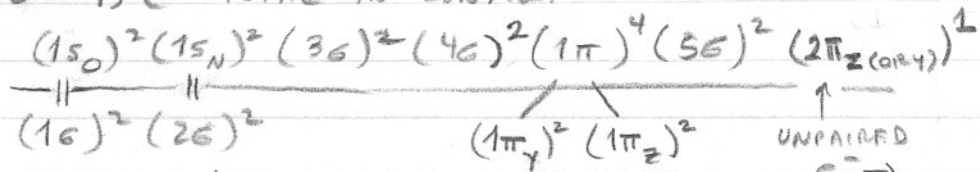
(c) From the last line above

$J_{1s\text{-valence}} \approx 23.3 \text{ eV}$

5

(d) Answer above.

[5.3] (a) NO - 15 e⁻ TOTAL IN CONFIG.



PARAMAGNETIC
MOLECULE
WITH $S = 1/2$

(b) For O 1s EMISSION: $\Delta E_b(O 1s) \propto K_{O 1s, 2\pi}$

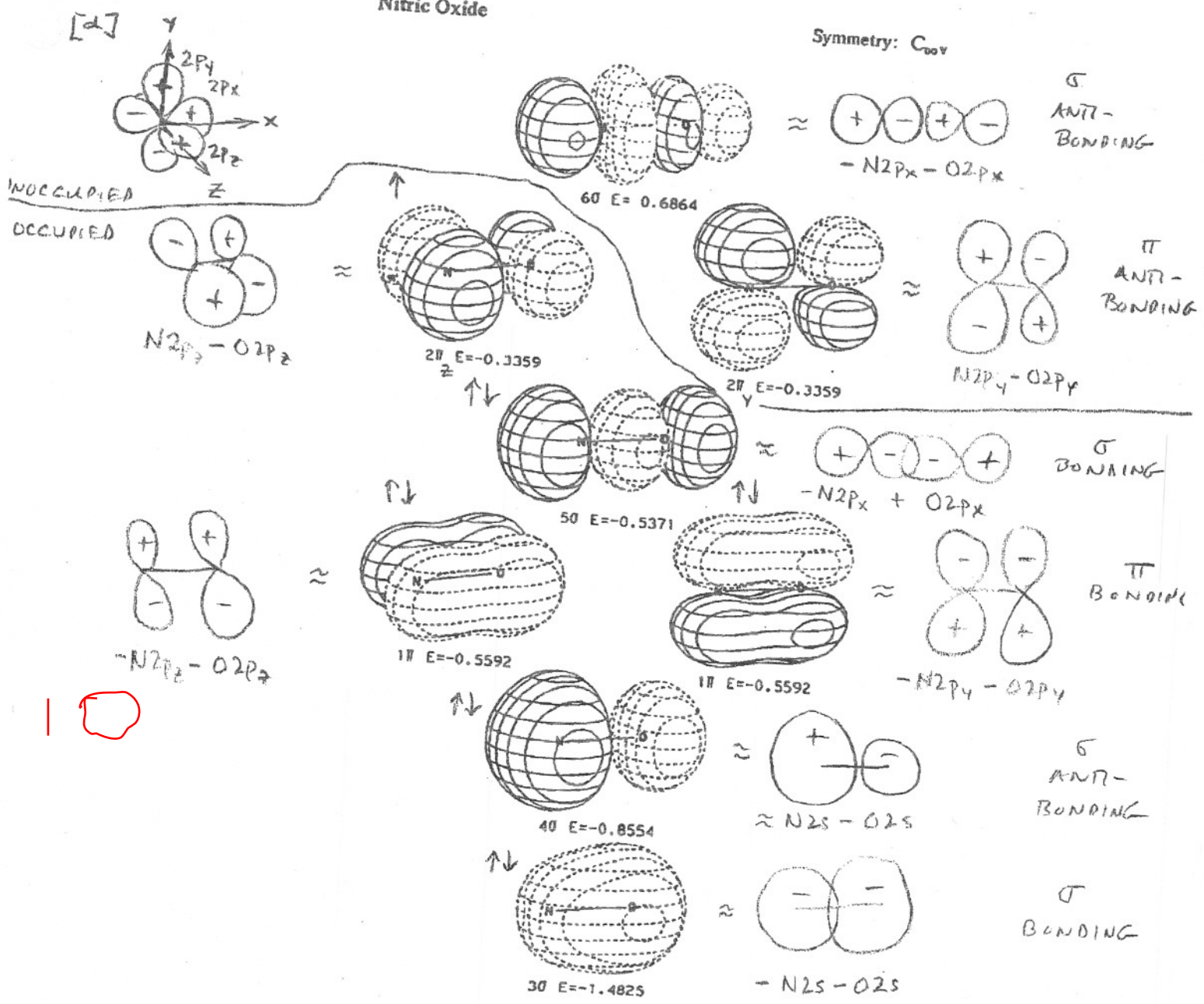
For N 1s EMISSION: $\Delta E_b(N 1s) \propto K_{N 1s, 2\pi}$

(c) 2 π MO IS MORE LOCALIZED ON N END OF
MOLECULE. THUS, $N 1s, 2\pi$ OVERLAP IS LARGER
AND $K_{N 1s, 2\pi}$ ALSO IS LARGER.



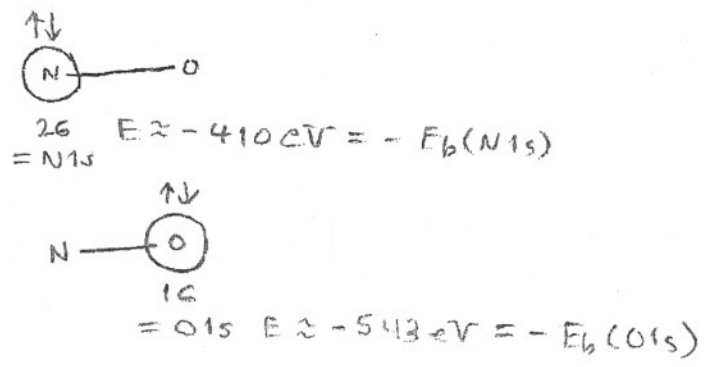
Nitric Oxide

Symmetry: $C_{\infty v}$



1

CORE LEVELS



[5.4]

5

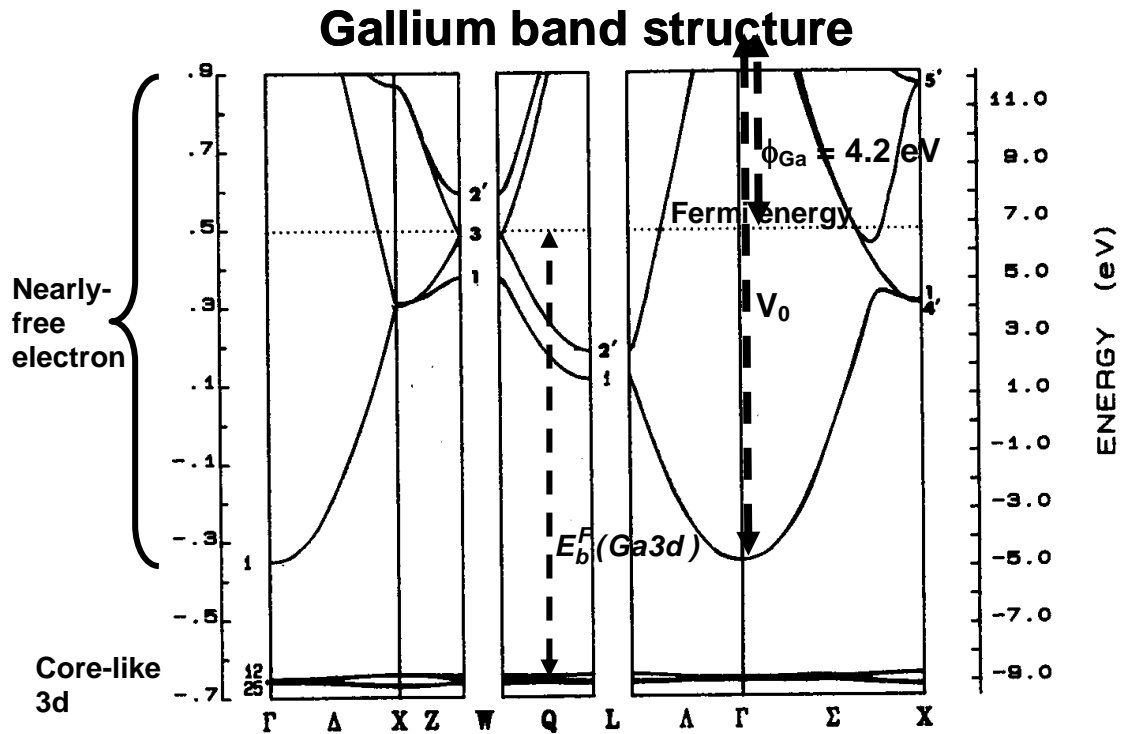
(a) The electron configuration of Ga is $3d^{10}4s^24p^1$. The 3d electrons are really core electrons, and the 4s and 4p occupation is like Ga's chemical relative Al with $3s^23p^1$. Not surprisingly, then, all of the bands above -5.0 eV are free-electron like, with splittings here and there due to the crystal potential, as in the nearly-free-electron model (e.g. Ashcroft and Mermin, pp. 152-173).

5

(b) These flat bands are the highly-localized, nearly-dispersionless, 3d bands of these core-like electrons. Checking the X-Ray Data Book for binding energy shows a Fermi-referenced 3d binding energy of 18.7 eV. The Fermi-referenced binding energy of these flat bands is $8.0 + 6.8 = 14.8$ eV, in good enough agreement with the tabulated value.

5

(c) With a work function of 4.0 eV (lecture slide) or 4.2 eV (from J. Phys.: Condens. Matter 10 (1998) 10815), the inner potential is from the bottom of the free-electron bands at -5.0 eV to the Fermi level, an energy of $5.0 + 6.8$, plus the work function of 4.2, to give $V_0 = 16$ eV.



[5.5] (a) Initially: $\Psi = \Psi_1 =$ grd. state ($n=1$) of particle in box of width l

$$\therefore = \left(\frac{2}{l}\right)^{1/2} \sin \frac{\pi x}{l} \text{ for } 0 \leq x \leq l; \text{ zero elsewhere } \textcircled{1}$$

$$E = E_1 = \frac{\hbar^2}{8ml^2}$$

After instantaneous change of box to width $2l$:

No wave function can change instantaneously; it must obey the t -dep. Schrodinger Egn., which has solutions continuous in time. Therefore, just after the change in box width, we still have

$$\Psi = \text{Eq. } \textcircled{1} \text{ above.}$$

However, the new set of allowed individual solutions to the t -indep. Schrod. Egn. are given by:

$$\Psi'_n = \left(\frac{2}{2l}\right)^{1/2} \sin\left(\frac{n\pi x}{2l}\right) \text{ for } 0 \leq x \leq 2l; \text{ zero elsewhere } \textcircled{2}$$

$$E'_n = n^2 \frac{\hbar^2}{8m(2l)^2} = \frac{n^2}{4} \left(\frac{\hbar^2}{8ml^2}\right), n=1,2,3,4,\dots \textcircled{3}$$

Expressing Ψ now as a linear combination of the complete set in $\textcircled{2}$ gives formally

$$\Psi = \sum_{n=1}^{\infty} a_n \Psi'_n$$

with a_n 's determined in usual way (see your favorite quantum mechanics book), from

$$a_n = \int_{-\infty}^{\infty} \Psi'_n \Psi dx = \int_0^l \left(\frac{1}{l}\right)^{1/2} \sin\left(\frac{n\pi x}{2l}\right) \left(\frac{2}{l}\right)^{1/2} \sin\left(\frac{\pi x}{l}\right) dx$$

↑
RANGE OF
NON-ZERO Ψ

$$= \frac{2^{1/2}}{l} \int_0^l \sin\left(\frac{n\pi x}{2l}\right) \sin\left(\frac{\pi x}{l}\right) dx = \frac{2^{1/2}}{l} \cdot \frac{l}{\pi} \int_0^l \sin\left(\frac{n\pi x}{2l}\right) \sin\left(\frac{\pi x}{l}\right) \frac{\pi dx}{l}$$

or, with change of variable to $u = \pi x/l$:

$$= \frac{2^{1/2}}{\pi} \int_0^{\pi} \sin\left(\frac{n u}{2}\right) \sin u du = \begin{cases} \text{if } n=2: \frac{2^{1/2}}{\pi} \cdot \frac{\pi}{2} = \frac{1}{2^{1/2}} \\ \text{if } n \neq 2: \frac{2^{1/2}}{\pi} \left[\frac{\sin\left(\frac{n}{2}-1\right)\pi}{2\left(\frac{n}{2}-1\right)} - \frac{\sin\left(\frac{n}{2}+1\right)}{2\left(\frac{n}{2}+1\right)} \right] \end{cases} \textcircled{4}$$

For $n \neq 2$, simplifying yields

$$a_n = \frac{2^{1/2}}{\pi} \left[\frac{(\frac{n}{2}+1) \sin(\frac{n}{2}-1)\pi - (\frac{n}{2}+1) \sin(\frac{n}{2}+1)\pi}{2(n^2/4-1)} \right],$$

plus with

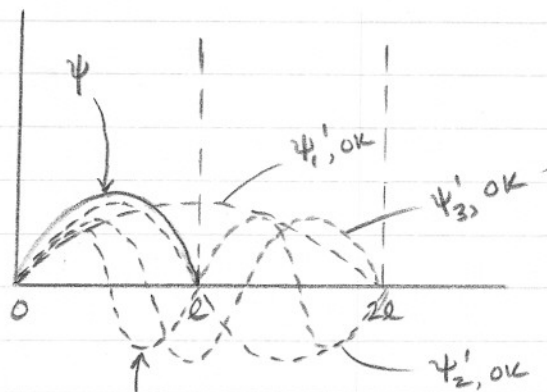
$$\sin(\frac{n}{2}-1)\pi = \sin(\frac{n}{2}+1)\pi \quad (\text{they are } 2\pi \text{ different in argument}),$$

and $\sin(\frac{n}{2}-1)\pi = -\sin(\frac{n\pi}{2}),$

$$a_n = -\frac{2^{1/2}}{\pi} \left[\frac{2 \sin(\frac{n\pi}{2})}{2(n^2/4-1)} \right] = -\frac{2^{1/2} \sin(\frac{n\pi}{2})}{\pi(n^2/4-1)} ; n \neq 2 \quad (5)$$

\therefore (4) + (5) dictate that a_n non-zero only for $n = 1, 2, 3, 5, 7, \dots$

Symmetry restriction against all even $n > 2$ easily seen from net overlaps in integral for a_n :



ψ_4' CANCELS AS + LOBE OF OVERLAP WITH $\psi = -$ LOBE.

ψ_6' LOOKS LIKE ψ_3 (INITIAL)

IN LEFT HALF AND SO ORTHOGONAL TO $\psi = \psi_1, \dots$ FOR ALL EVEN $n > 2$.

\therefore overall

$$\psi = \psi_1 = \frac{1}{(2l)^{1/2}} \sin\left(\frac{\pi x}{2l}\right) + \sum_{n=1,3,5}^{\infty} \left(\frac{2^{1/2} \sin(\frac{n\pi}{2})}{\pi(n^2/4-1)l^{1/2}} \right) \sin\left(\frac{n\pi x}{2l}\right)$$

(b) The average energy will be given by:

$$\langle E \rangle = \sum_{n=1}^{\infty} |a_n|^2 E_n'$$

where $|a_n|^2 =$ probability of measuring the energy

E_n' associated with the first state eigenfunction ψ_n' . Thus, we have:

$$\langle E \rangle = |a_2|^2 E_2 + \sum_{n=1,3,5,\dots}^{\text{ODD}} |a_n|^2 E_n$$

$$= \frac{\hbar^2}{8mL^2} \left[\frac{1}{2} + \sum_{n=1,3,\dots} \frac{2 \sin^2(n\pi/2)}{\pi^2 (n^2/4 - 1)^2} \cdot \frac{n^2}{4} \right]$$

$$= \frac{\hbar^2}{8mL^2} \left[\frac{1}{2} + \sum_{n=1,3,\dots}^{\infty} \frac{16 n^2}{2\pi^2 (n^2 - 4)^2} \right]$$

$$= E_1 \left[\frac{1}{2} + \frac{8}{\pi^2} \sum_{n=1,3,5,\dots} \frac{n^2}{(n^2 - 4)^2} \right]$$

Always +1, since squared.
 a standard series = $\frac{\pi^2}{16}$

$$= E_1 \left[\frac{1}{2} + \frac{1}{2} \right]$$

$$= \underline{\underline{E_1}}, \text{ Q.E.D.}$$

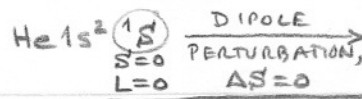
Thus, although each measurement of E may yield any one of the E_n' values, the average over a large number of measurements will give the same energy as before the sudden expansion of the box.

(2) This problem thus has 1:1 correspondences to the Sudden Approximation in photoemission as:

	THIS PROBLEM	CORE PHOTOE ⁻ EMISSION
①	SUDDEN CHANGE IN \hat{V} BOX(L) → BOX(2L)	EMISSION OF CORE e ⁻ TO FORM k HOLE
②	INITIAL ψ ψ IN BOX(L)	(N-1)e ⁻ ψ_R IN INITIAL N e ⁻ \hat{H}
③	FINAL ψ_j 's ψ_n' IN BOX(2L)	(N-1)e ⁻ ψ_j^f OF ACTUAL ION (k-hole)
④	PROBAB. OF ψ_j $ \int \psi_n' \psi dx ^2$	$ \int \psi_j^f \psi_R dV ^2 = \langle \psi_j^f(N-1) \psi_R(N-1) \rangle ^2$
⑤	CONSTANCY OF ⟨ENERGY⟩ ⟨E⟩ = E ₁	"HANNE-ÅBERG" OR "HEDIN-LUNDQVIST" THEOREM: (AVER. E ₀ OVER ALL PEAKS) = -E _k = KOOPMANS' RESULT

[5.6]

Overall transition is:



relaxed photoe⁻: Taken arbitrarily to be $l=0, m_l=+1, (P) (+1)$
 $\text{He } 1s', E_{P+1}^F \begin{matrix} (1P) \\ S=0 \\ L=1, M_L=+1 \end{matrix}$
 one choice allowed by dipole selection rule.

N. A.

(a) The $1S$ ground state of $\text{He } 1s^2$ is, in a Slater determinant approximation (see your favorite q.m. book):

$$\psi^i(2) = \frac{1}{\sqrt{2}} \begin{vmatrix} 1s(1)\alpha(1) & 1s(1)\beta(1) \\ 1s(2)\alpha(2) & 1s(2)\beta(2) \end{vmatrix}$$

$$= 1s(1)1s(2) \cdot \frac{1}{\sqrt{2}} [\alpha(1)\beta(2) - \beta(1)\alpha(2)] \quad (1)$$

The $S=0$ spin function for $2e^-$.

(b) The final state must also be a singlet state (with $S=0$), because the dipole operator cannot change spin. Thus, its $2-e^-$ spin function must be the same as that in (1). The new total configuration is different however, in having electrons in 2 inequivalent orbitals. I.e., the overall $2-e^-$ configuration is $\text{He}^+ + \text{photoe}^- = 1s'(\text{relaxed}), E_{P+1}^F$, where the photoelectron is at energy E_F , with $l=1, m_l=1$, as stated in problem. The wave function here must be a sum of two Slater determinants in order to yield the correct $S=0$ state (see your q.m. book again):

$$\psi^f(2) = \frac{1}{\sqrt{2}} \left[\frac{1}{\sqrt{2}} \begin{vmatrix} 1s'(1)\alpha(1) & E_{P+1}^F(1)\beta(1) \\ 1s'(2)\alpha(2) & E_{P+1}^F(2)\beta(2) \end{vmatrix} - \frac{1}{\sqrt{2}} \begin{vmatrix} 1s'(1)\beta(1) & E_{P+1}^F(1)\alpha(1) \\ 1s'(2)\beta(2) & E_{P+1}^F(2)\alpha(2) \end{vmatrix} \right]$$

MANY PEOPLE MISS THIS PIECE.

$$= \frac{1}{\sqrt{2}} \left[\underbrace{1s'(1)E_{P+1}^F(2) + E_{P+1}^F(1)1s'(2)}_{\text{SYMMETRIC}} \right] \cdot \frac{1}{\sqrt{2}} \underbrace{[\alpha(1)\beta(2) - \beta(1)\alpha(2)]}_{\text{ANTI-SYMMETRIC}} \quad (2)$$

$S=0$ spin function

The matrix element desired is thus:

$$\langle \Psi^f(\mathbf{r}_1, \mathbf{r}_2) | \Psi^i(\mathbf{r}_1, \mathbf{r}_2) \rangle = \langle \frac{1}{\sqrt{2}} [1s^f(1) E_{P+1}^f(2) + E_{P+1}^f(1) 1s^f(2)] | \frac{S=0}{\text{spin}} | \mathbf{r}_1, \mathbf{r}_2 | 1s(1) 1s(2) \cdot \frac{S=0}{\text{spin}} \rangle$$

Integration on two spin coordinates σ_1 and σ_2 gives $\underline{1}$, because $S=0$ function is unnormalized.

Integration on two spin coordinates can be done separately, since $\mathbf{r}_1, \mathbf{r}_2$ does not affect them; this yields $\underline{1}$, as indicated above.

Remaining spatial integrals can now be evaluated by expanding products and noting \mathbf{r}_1 affects dV_1 integration only and \mathbf{r}_2 affects dV_2 integration only. This yields:

$$\begin{aligned} \langle \Psi^f(\mathbf{r}_1, \mathbf{r}_2) | \Psi^i(\mathbf{r}_1, \mathbf{r}_2) \rangle &= \frac{1}{\sqrt{2}} \left\{ \langle 1s^f(1) E_{P+1}^f(2) | \mathbf{r}_1 | 1s(1) 1s(2) \rangle \right. \\ &\quad + \langle 1s^f(1) E_{P+1}^f(2) | \mathbf{r}_2 | 1s(1) 1s(2) \rangle \\ &\quad + \langle E_{P+1}^f(1) 1s^f(2) | \mathbf{r}_1 | 1s(1) 1s(2) \rangle \\ &\quad \left. + \langle E_{P+1}^f(1) 1s^f(2) | \mathbf{r}_2 | 1s(1) 1s(2) \rangle \right\} \end{aligned}$$

Or, separating dV_1 and dV_2 integrations into products:

$$\begin{aligned} &= \frac{1}{\sqrt{2}} \left\{ \begin{array}{l} \textcircled{1} \cdot \textcircled{2} \\ \langle 1s^f(1) | \mathbf{r}_1 | 1s(1) \rangle \langle E_{P+1}^f(2) | 1s(2) \rangle \\ + \textcircled{3} \cdot \textcircled{4} \\ \langle 1s^f(1) | 1s(1) \rangle \langle E_{P+1}^f(2) | \mathbf{r}_2 | 1s(2) \rangle \\ + \textcircled{5} \cdot \textcircled{6} \\ \langle E_{P+1}^f(1) | \mathbf{r}_1 | 1s(1) \rangle \langle 1s^f(2) | 1s(2) \rangle \\ + \textcircled{7} \cdot \textcircled{8} \\ \langle E_{P+1}^f(1) | 1s(1) \rangle \langle 1s^f(2) | \mathbf{r}_2 | 1s(2) \rangle \end{array} \right\} \quad \textcircled{3} \end{aligned}$$

This is easily simplified by recalling certain orthogonality relations among the orbitals. I.e., the orbitals all can be written as:

$$1s(\vec{r}) = R_{1s}(r) Y_0^0(\theta, \phi)$$

$$1s'(\vec{r}) = R'_{1s}(r) Y_0^0(\theta, \phi)$$

$$E_{P+1}^f(\vec{r}) = R_{E_{P+1}^f}(r) Y_1^1(\theta, \phi).$$

Therefore, integrals (2) and (7) in Eq. (3) are zero, because Y_0^0 and Y_1^1 are orthogonal when integrated over all θ and ϕ . By a similar argument, integrals (1) and (8) are also zero. $1s'(\vec{r}) \cdot 1s(\vec{r})$ is an even function of \vec{r} , but \vec{r} itself is odd; thus the overall integrand is odd and integrates to zero.

Also, in integrals (3) - (6), once the dV_1 and dV_2 integrals are separated, the labels 1 and 2 can be interchanged. Thus, (3) = (6) and (4) = (5), and we have finally

$$\langle \Psi^f(2) | \vec{r}_1 + \vec{r}_2 | \Psi^i(2) \rangle = \sqrt{2} \langle E_{P+1}^f | \vec{r} | 1s \rangle \langle 1s' | 1s \rangle. \quad (4)$$

This is indeed equivalent to Eq. (68) in Λ , with the identifications:

$$\begin{aligned} \phi^f &= E_{P+1}^f & ; & & \psi^f(N-1) &= \psi^f(1) = 1s' \text{ (relaxed)}; \\ \phi_k &= 1s & ; & & \psi_k(N-1) &= \psi_k(1) = 1s. \end{aligned}$$

The extra factor of $\sqrt{2}$ relative to Eq. (68) comes about because two Slater dets. are involved in the final state. This extra factor has a simple physical significance that can be seen by noting that the intensity of the $\Psi^i(2) \rightarrow \Psi^f(2)$ excitation will be proportional to the square of Eq. (4) or

$$I \propto |\langle \Psi^f(z) | \vec{r}_1 + \vec{r}_2 | \Psi^i(z) \rangle|^2 = \underline{2} \cdot |\langle E_{p+1}^f | \vec{r} | 1s \rangle|^2 |\langle 1s' | 1s \rangle|^2. \quad (5)$$

I.e., the intensity seems to be twice that expected for a simple $1s \rightarrow E_{p+1}^f$ transition with $1s$ relaxing to $1s'$. However, if we look back at the two determinants (A) and (B) in Eq. (2) for $\Psi^f(z)$, we can see that (A) represents a $1s\beta \rightarrow E_{p+1}\beta$ transition, whereas (B) represents a $1s\alpha \rightarrow E_{p+1}\alpha$ transition. (Recall that $1-e^-$ spin cannot change either.) Thus, the factor 2 represents a unit of intensity for either the spin up excitation channel or the spin down channel, which act independently so as to add to 2. If we were to detect photoelectron spin somehow, the final state would have to be modified so as to project out only one spin, and the intensity would be reduced to $1/2$ of Eq. (5).

(c) $He^+ 1s'$ is just a hydrogenic atom with $Z=2$. So

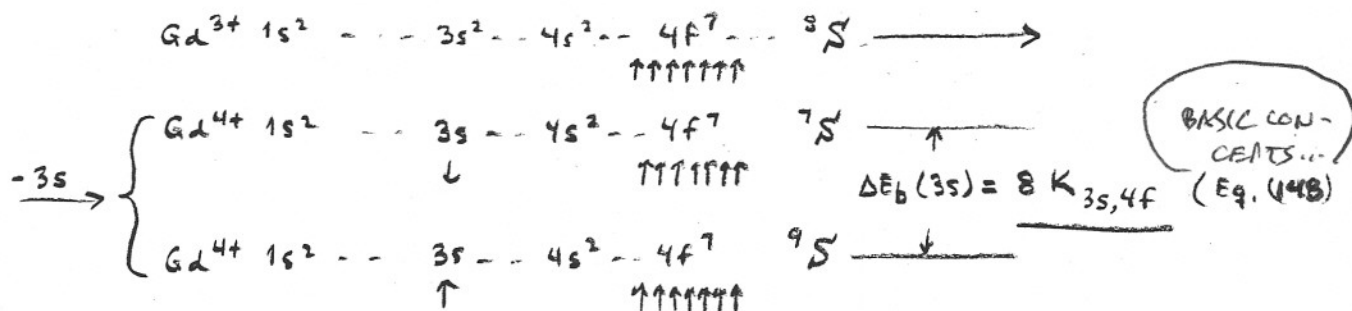
$$\psi_{1s'} = \psi_{1s}(Z=2).$$



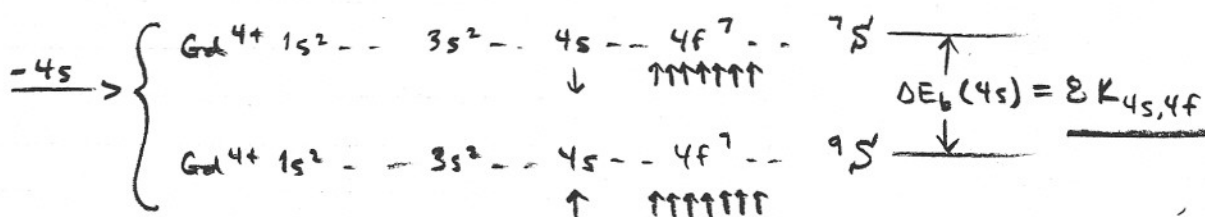
-100

[5.7] (a) All subshells initially filled except 4f⁷, so we can write 3s emission as

20 points



or, with 4s emission as

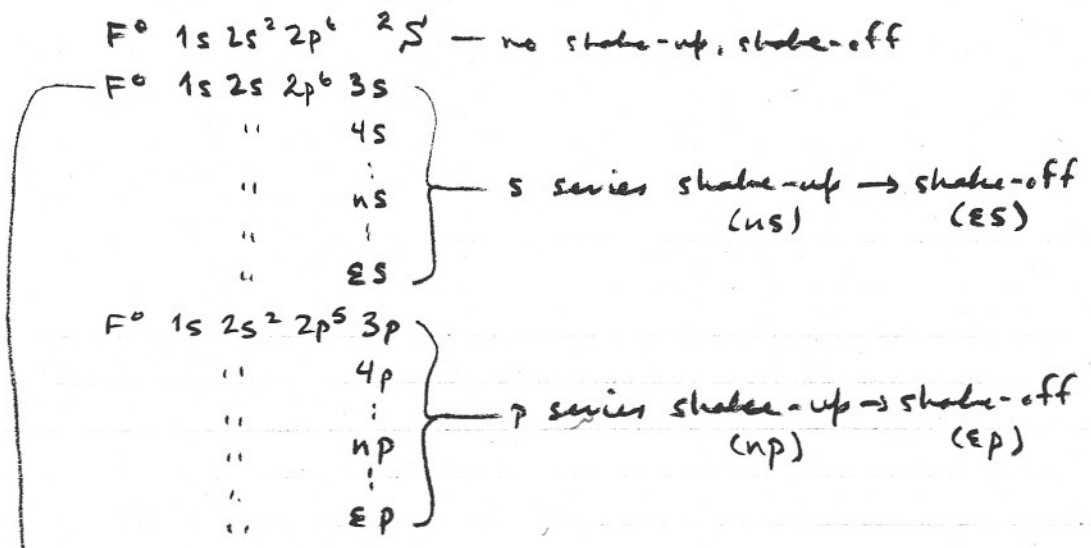


with in both cases on intensity ratio of

$$\frac{I(7s)}{I(9s)} = \frac{7}{9} \quad (\text{Eq. (44)})$$

- (b) 4s, because 4s and 4f electrons overlap more and therefore $K_{4s,4f} > K_{3s,4f}$.
- (c) 3s more accurately predicted by simple HF theory, because the higher overlap of 4s and 4f leads to greater e⁻e⁻ correlation corrections in the uncorrelated 7s state. (Recall that exchange correlates the spin-parallel electrons in the 9s states somewhat.)
- (d) No multiplet splitting, because the F⁻ ions have an inert-gas valence configuration. So, no net valence spin to couple remaining 1s electron with.

(e) Easy to do if we note that e^- configuration is identical to neon example of lecture and "Basic Concepts...". So, The final F^0 states are like:



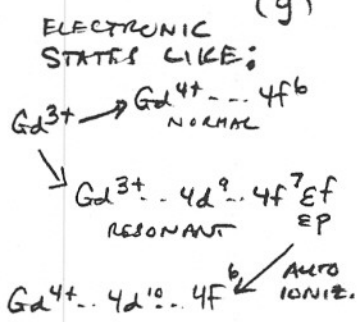
→ With overlaps for this typical case like:

$$I \propto \langle \underbrace{1s 2s 2p^6}_{\text{Relaxed}} \underbrace{3s}_{9-e^-} | \underbrace{1s 2s^2 2p^6}_{\text{Initial}} \rangle^2 = \langle 1s | 1s \rangle \langle 2s | 2s \rangle \langle 3s | 2s \rangle \cdot$$

$$\langle 2p_x | 2p_x \rangle \langle 2p_y | 2p_y \rangle \langle 2p_z | 2p_z \rangle \langle 2p_x | 2p_y \rangle \langle 2p_y | 2p_z \rangle \langle 2p_z | 2p_x \rangle$$



(f) Cooper minima evident for Gd 4d at $h\nu \approx 220 \text{ eV}$ and for Gd 5d at $h\nu \approx 155 \text{ eV}$.



(g) Gd 4f may exhibit resonant photoemission with the Gd 4d shell just adjacent to it in spatial extent and binding energy. This would be expected to occur at $h\nu \approx$ Gd 4d BINDING ENERGY $\approx 128 \text{ eV}$ (VALUE OF 162.0 eV IN YEH + LINDAU IS CALCULATED, AND SO IN ERROR BY δE_{RELAX} ETC.)

(h) E_{KIN} VALUES FOR ALL THREE VALANCE SUBSHELLS ESSENTIALLY EQUAL, SINCE $E_b \ll h\nu = 1486 \text{ eV}$. THUS, WE CAN FORGET ALL ENERGY-DEPENDENT ANALYZER FACTORS ($A_0 R_0 D_0$). ALSO, ALL e^- ARE FROM SAME ATOM, SO ATOMIC DENSITIES ARE EQUAL, MEAN FREE PATHS ARE ALSO EQUAL, SINCE E_{KIN} VALUES SO CLOSE.

∴ ALL THIS LEAVES US A RATIO OF SUBSHELL DIFFERENTIAL CROSS SECTIONS:

$$I_{4f} : I_{5d} : I_{6s} = \frac{d\sigma_{4f}}{d\Omega} : \frac{d\sigma_{5d}}{d\Omega} : \frac{d\sigma_{6s}}{d\Omega}$$

$$= \sigma_{4f} \left[1 + \frac{1}{2} \beta_{4f} \left(\frac{3}{2} \sin^2 \alpha - 1 \right) \right] : \sigma_{5d} \left[1 + \frac{1}{2} \beta_{5d} \left(\frac{3}{2} \sin^2 \alpha - 1 \right) \right] : \sigma_{6s} \left[1 + \frac{1}{2} \beta_{6s} \left(\frac{3}{2} \sin^2 \alpha - 1 \right) \right]$$

FOR ALL THREE
- 0.1198

YEH + LINDAU TABLES

$$\downarrow$$

$$= 0.021 \left[1 - \frac{1}{2} (1.039) (0.1198) \right] : 0.00094 \left[1 - \frac{1}{2} (1.388) (0.1198) \right] : 0.00043 \left[1 - \frac{1}{2} (2.000) (0.1198) \right]$$

ALL 5 SUBSHELLS

$$= 0.0197 : 0.000862 : 0.000378 = \underline{1.000 : 0.044 : 0.019}$$

SO, VERY LITTLE OF 5d AND 6s INTENSITY SEEN IN XPS OF Gd (OR OTHER RARE EARTHS).

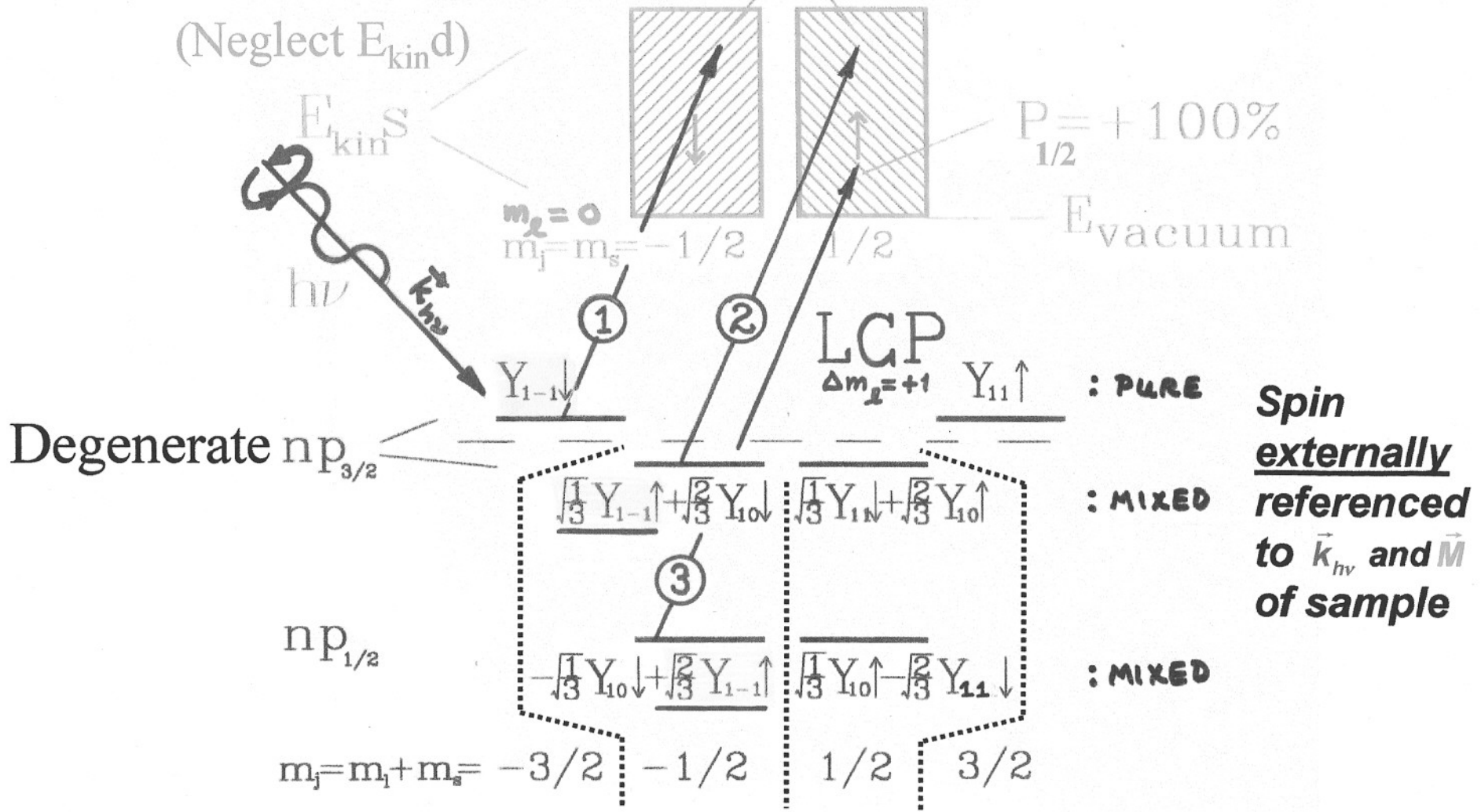
and $\Delta m_e = -1$.

(i) Just use reasoning in following example discussed in lecture, but spins reversed since RCP. This gives $\tau = +50\%$



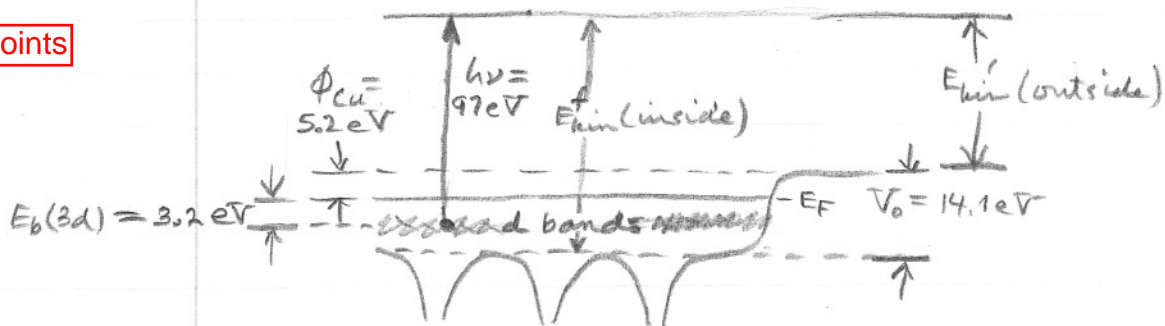
PHOTOELECTRON SPIN POLARIZATION FROM CIRCULAR POLARIZATION AND SPIN-ORBIT SPLITTING (THE FANO EFFECT)

$$P_{3/2} = -50\% = \frac{\sqrt{1/3^2 - 1^2}}{\sqrt{1/3^2 + 1^2}} \times 100 = \frac{-2/3}{4/3} \times 100 = -50\%$$



[5.8] Relevant energy + potential diagram is:

15 points

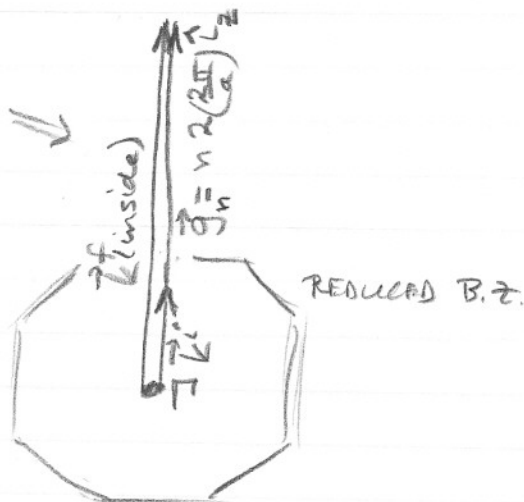


(a) From diagram, $E_{min}^f(\text{inside}) = 97 \text{ eV} + (14.1 - 5.2 - 3.2) \text{ eV}$
 $= 97 \text{ eV} + 5.7 \text{ eV}$
 $= 102.7 \text{ eV}$

$\therefore |\vec{k}^f(\text{inside})| = 0.512 [102.7]^{0.5}$
 $= 5.189 \text{ \AA}^{-1}$

and \vec{k} conservation looks like:

$\vec{k}^f(\text{inside})$
 $= \vec{k}^i(\text{in RBZ}) + \vec{g}_n$



Assume $n=1$ for \vec{g} as first try:

$|\vec{g}_1| = 2 \left(\frac{2\pi}{a} \right) = \frac{4\pi}{3.61 \text{ \AA}} = 3.481 \text{ \AA}^{-1}$

$\therefore |\vec{k}^i| = |\vec{k}^f(\text{inside})| - |\vec{g}_1| = 5.189 \text{ \AA}^{-1} - 3.481 \text{ \AA}^{-1}$
 $= 1.708 \text{ \AA}^{-1}$

But X point is at $\frac{2\pi}{a}$ along \vec{z} direction $= \frac{2\pi}{3.61} = 1.741 \text{ \AA}^{-1}$
 or very close to $|\vec{k}^i|$ for 97 eV excitation.

(b) Just outside the surface, \bar{V}_0 is lost to give $102.7 \text{ eV} - 14.1 \text{ eV} = \underline{\underline{88.6 \text{ eV}}}$

(c) $P_{hv} = \hbar k_{hv} = \frac{h}{\lambda}$ (de Broglie rel'n.)

$\therefore k_{hv} = \frac{2\pi}{\lambda_{hv}}$ (the usual relationship)

For $h\nu = 97 \text{ eV}$, $\lambda_{hv} = \frac{12,398}{97} = 127.8 \text{ \AA}$, so

$$k_{hv} = \frac{2\pi}{127.8} = 0.0492 \text{ \AA}^{-1}$$

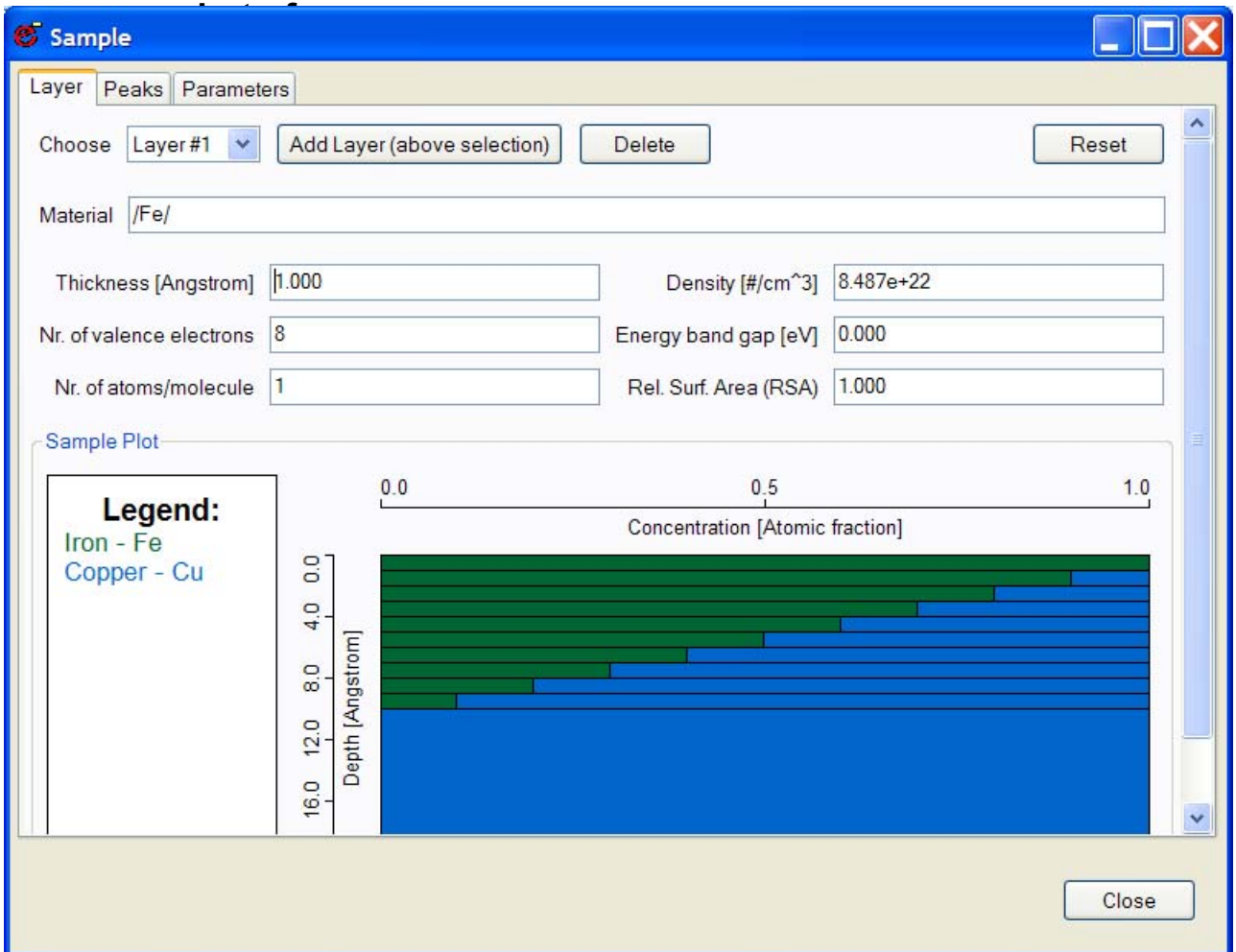
which is very small compared to the rB^7 radius of 1.708 \AA^{-1} (only about 3%), and so negligible.

[5.9.]

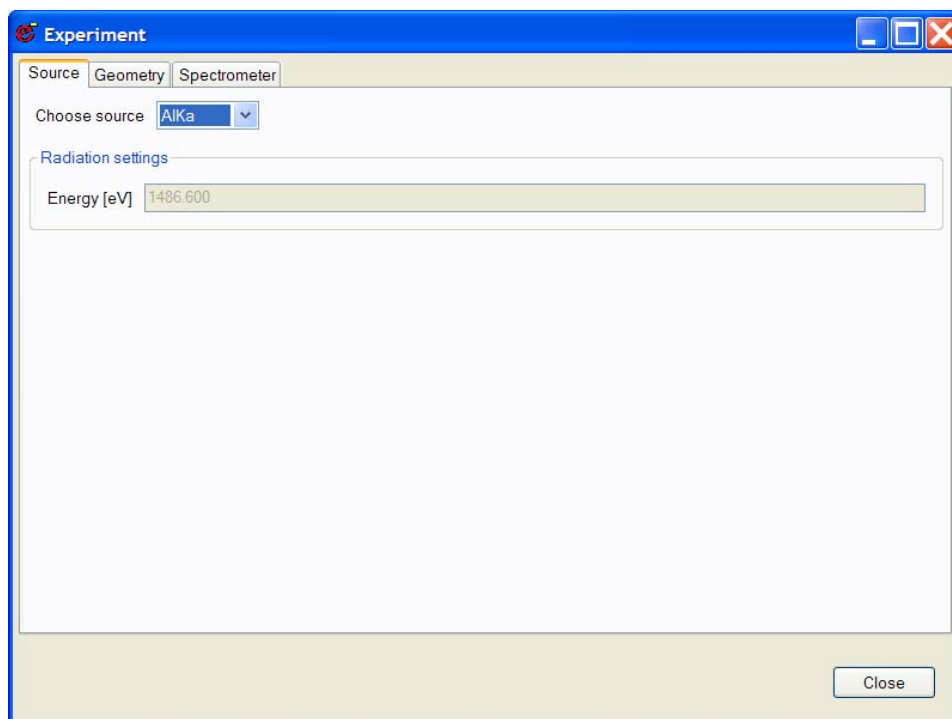
(a) Average no. electrons for Fe and Cu is $(11+8)/2 = 9.5$, but SESSA requires integers, so could use 9.0 or 10.0. I'll use 10 for the mixed layers.

20 points

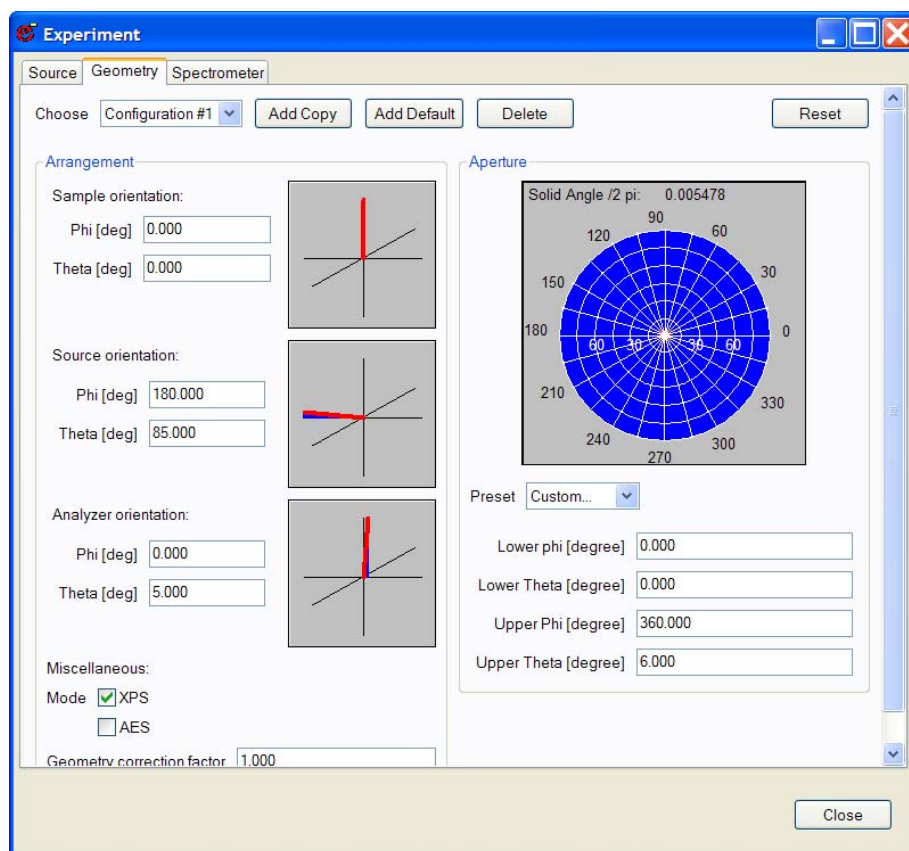
Average atomic density is $(8.50+8.45)/2 \times 10^{22} = 8.48 \times 10^{22}$.
Building up the sample from Cu substrate plus ten layers of Fe+Cu from /Fe10/Cu90/ to /Fe20/Cu80/ to /Fe30/Cu70/,...to /Fe/ yields finally



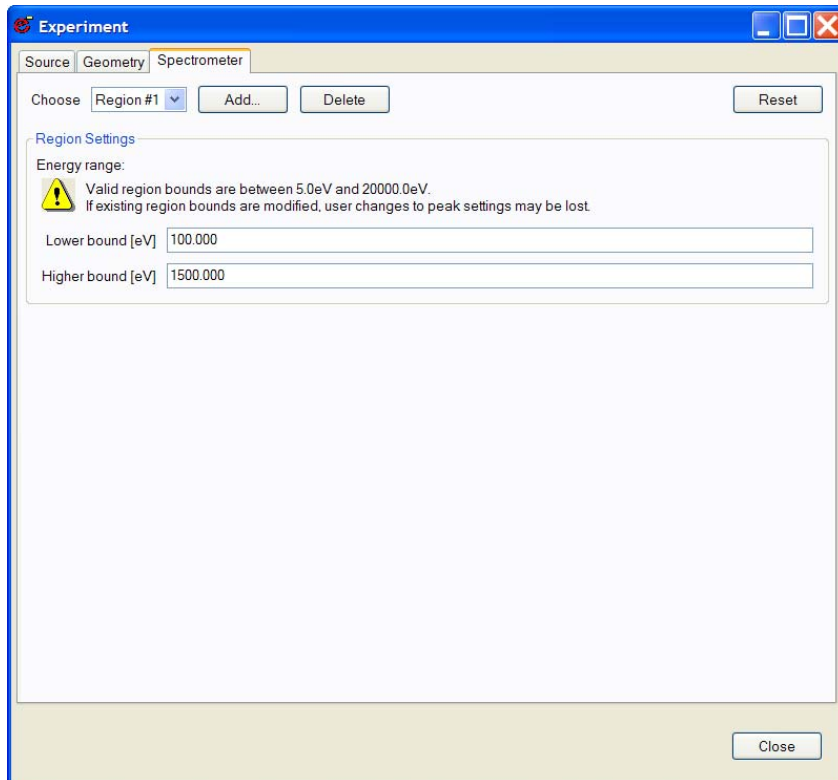
The source is just the default $AlK\alpha$ in the program, as shown in the screen shot on the next page.



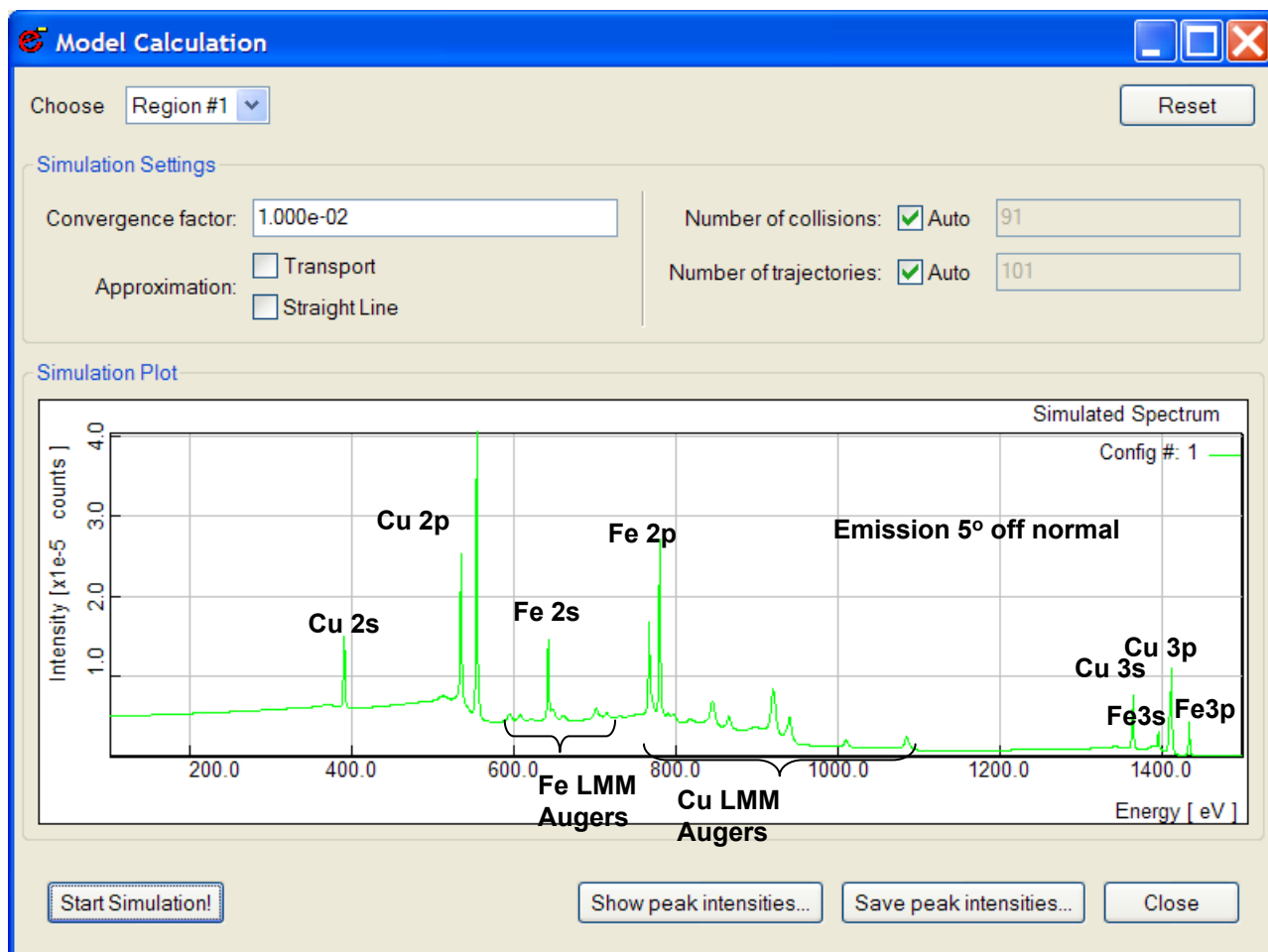
The geometry is as shown below:

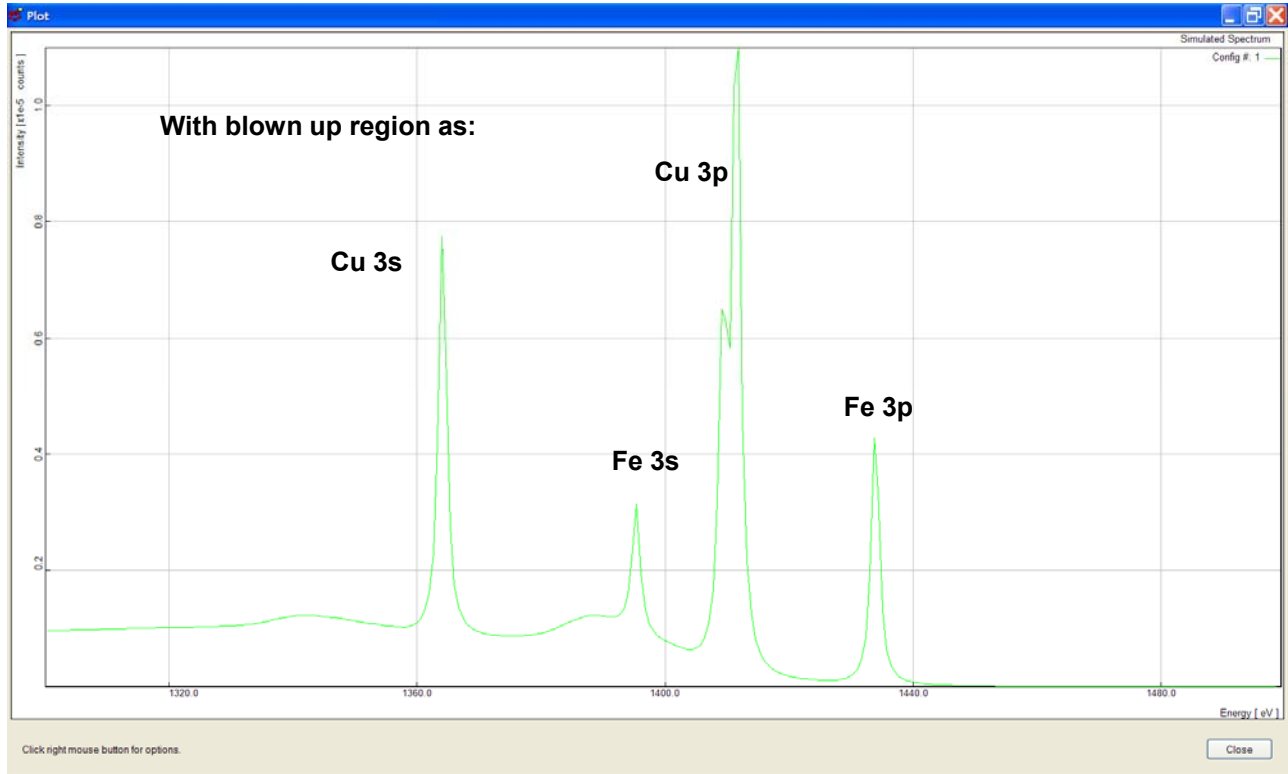


The spectrometer is defined as below:

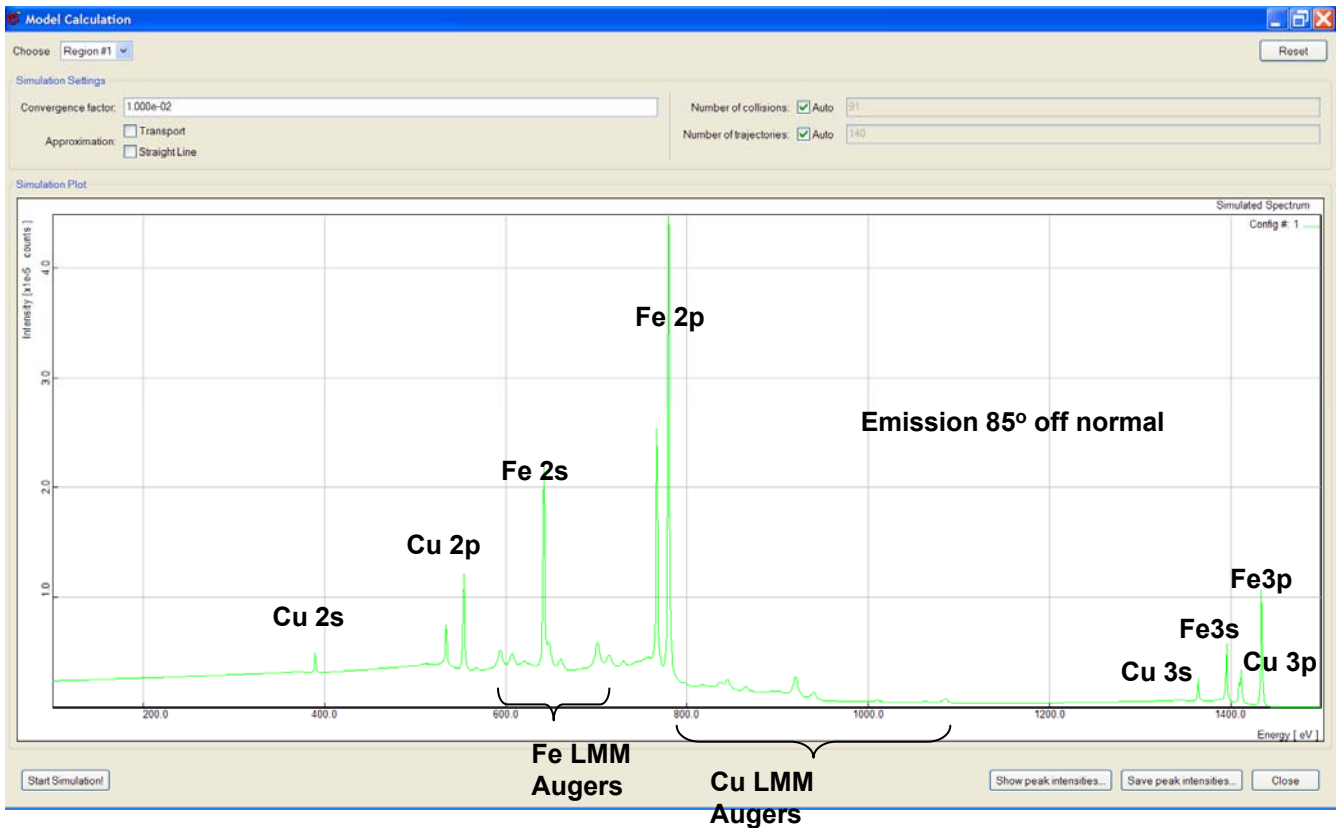


The result of the simulation is then:





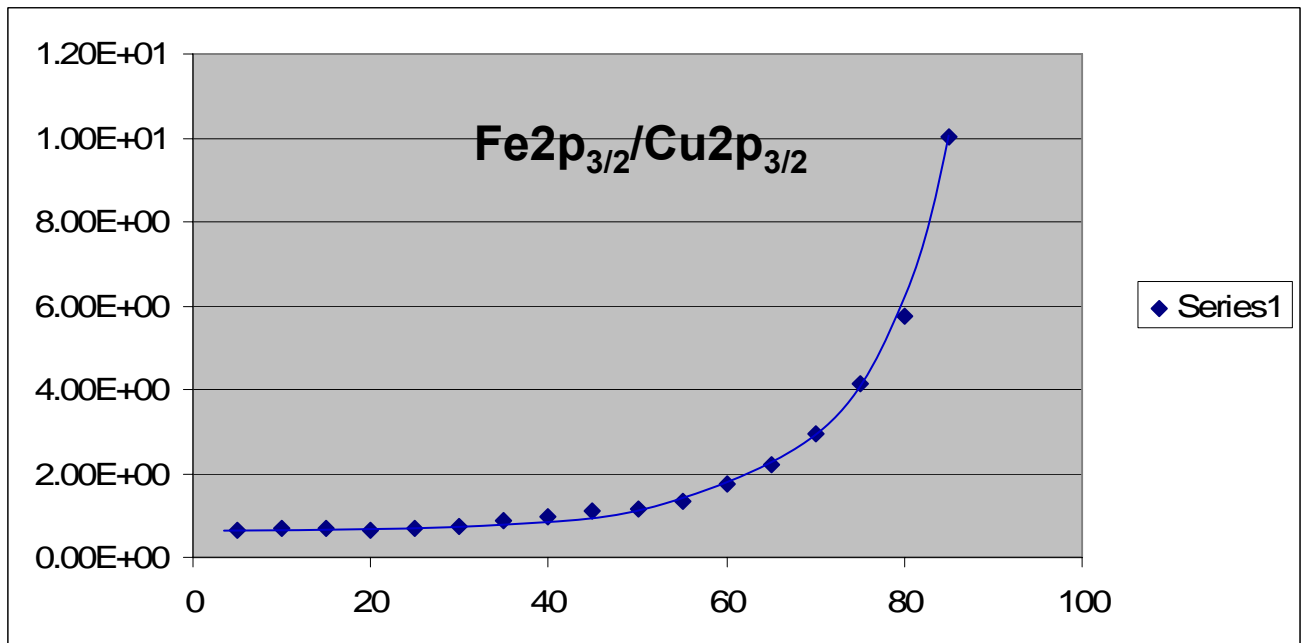
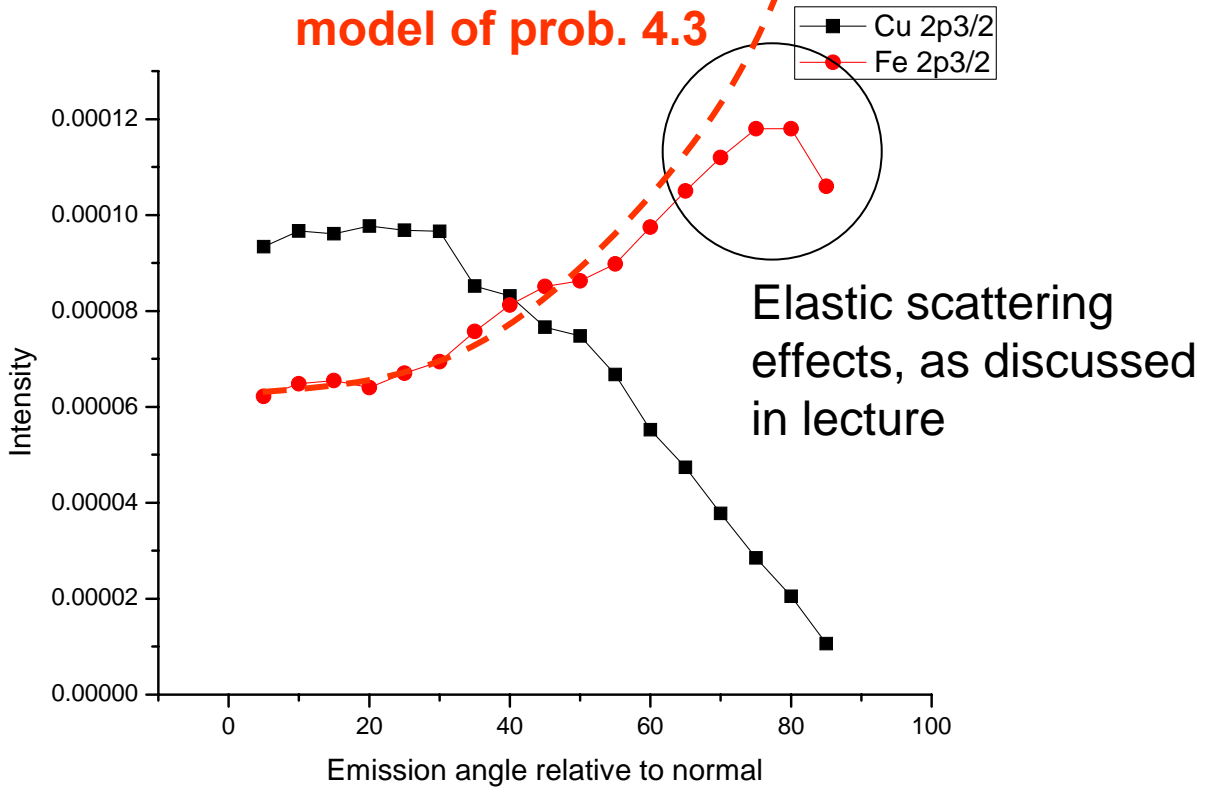
Changing only the takeoff angle to now be 85 deg.off normal = 5 degree takeoff angle dramatically enhances all Fe features:



(b) Calculating Cu 2p_{3/2} and Fe 2p_{3/2} intensities now for the different angles requested now yields:

Electron emission angle (w.r.t. normal)	Cu 2p _{3/2}	Fe 2p _{3/2}	Fe2p _{3/2} / Cu2p _{3/2}
85	1.06009e-05	1.06205e-04	1.00E+01
80	2.05254e-05	1.18011e-04	5.74951
75	2.84874e-05	1.18007e-04	4.142428
70	3.77737e-05	1.11802e-04	2.959784
65	4.73596e-05	1.04910e-04	2.215179
60	5.52105e-05	9.75318e-05	1.766544
55	6.67060e-05	8.98120e-05	1.346386
50	7.47551e-05	8.63412e-05	1.154987
45	7.65899e-05	8.50740e-05	1.110773
40	8.31061e-05	8.11802e-05	0.976826
35	8.52360e-05	7.57348e-05	0.888531
30	9.65751e-05	6.94172e-05	0.71879
25	9.67727e-05	6.70305e-05	0.692659
20	9.76668e-05	6.40239e-05	0.655534
15	9.60796e-05	6.55382e-05	0.682124
10	9.67096e-05	6.47569e-05	0.669602
5	9.33935e-05	6.21533e-05	0.665499

More what's expected,
from the simple
model of prob. 4.3



Marked enhancement
of Fe relative intensity for
more grazing angles of
emission

(c) The expected angular variation of Fe 2p_{3/2} is from the answer for problem 4.3 according to:

$$\left\{ 1 + \frac{\Lambda_e \sin \theta}{z_0} \left(e^{-z_0 / \Lambda_e \sin \theta} - 1 \right) \right\}$$

But with θ defined as the complement in the SESSA program. So this part of the problem involves calculating this function with $z_0 = 10 \text{ \AA}$, and $\Lambda_e = 13 \text{ \AA}$ = an average no. from the "Parameters" list in SESSA for the Fe 2_{3/2} peak, which gives:

$$1 + \frac{13 \cos \theta}{10} \left[\exp\left(-\frac{10}{13 \cos \theta}\right) - 1 \right] = 1 + 1.3 \cos \theta \left[\exp(-0.769 / \cos \theta) - 1 \right]$$

which has limits of 0.300 for $\theta = 5^\circ$ (where the simple model is expected to be better) and 1.11 for $\theta = 85^\circ$ or a factor of 3.7 enhancement at more grazing emission angles. However, the actual change over this range from SESSA is only about 1.7, so the effects of elastic scattering are important, particularly over the circled region of the red curve. You could go further and normalize experiment to simple theory at $\theta = 5^\circ$ and the plot them together, to see where they begin to diverge.

Running SESSA in a "straight-line" trajectory mode to should reduce the effects of elastic scattering in taking intensity away from a given initial emission direction, and leads to:

	$\theta = 85^\circ$	$\theta = 5^\circ$	85/5 ratio
Fe 2p _{3/2}	1.57476e-04	5.89509e-05	2.67
	(1.7 from full SESSA, 3.7 from simple model)		
Cu 2p _{3/2}	1.08118e-05	1.34945e-04	0.089
	(0.113 from full SESSA).		

So two calculations for Fe close up a little this way, but deviations from simple model still persist.

[5.10]

20 points

(a) Mn^{2+} is in an octahedral environment of O^{2-} ions in the NaCl crystal structure, and we can just go to the CTM4XAS manual posted at the website to get the relevant parameters. We'll add a crystal field splitting of 1.0 eV beyond the sample calculations done in our manual, so that the input formats for XAS looks like:

The screenshot shows the CTM4XAS 2.0 software interface. The window title is "Figures - CTM4XAS 2.0". The menu bar includes "Calculate", "Plot", "Debug", "Desktop", "Window", and "Help".

Configuration:

- Ion:
- Auto Plot
- XPS
- Charge transfer
- Initial state: Initial state (CT):
- Final state: Final state (CT):
- Slater integral reduction (%): Fdd: Fpd: Gpd:
- 3d spin-orbit:
-
- Expert options

Crystal field parameters (eV):

- Symmetry:
- Initial state: Final state
- 10 Dq:
- Dt:
- Ds:
- M (meV):

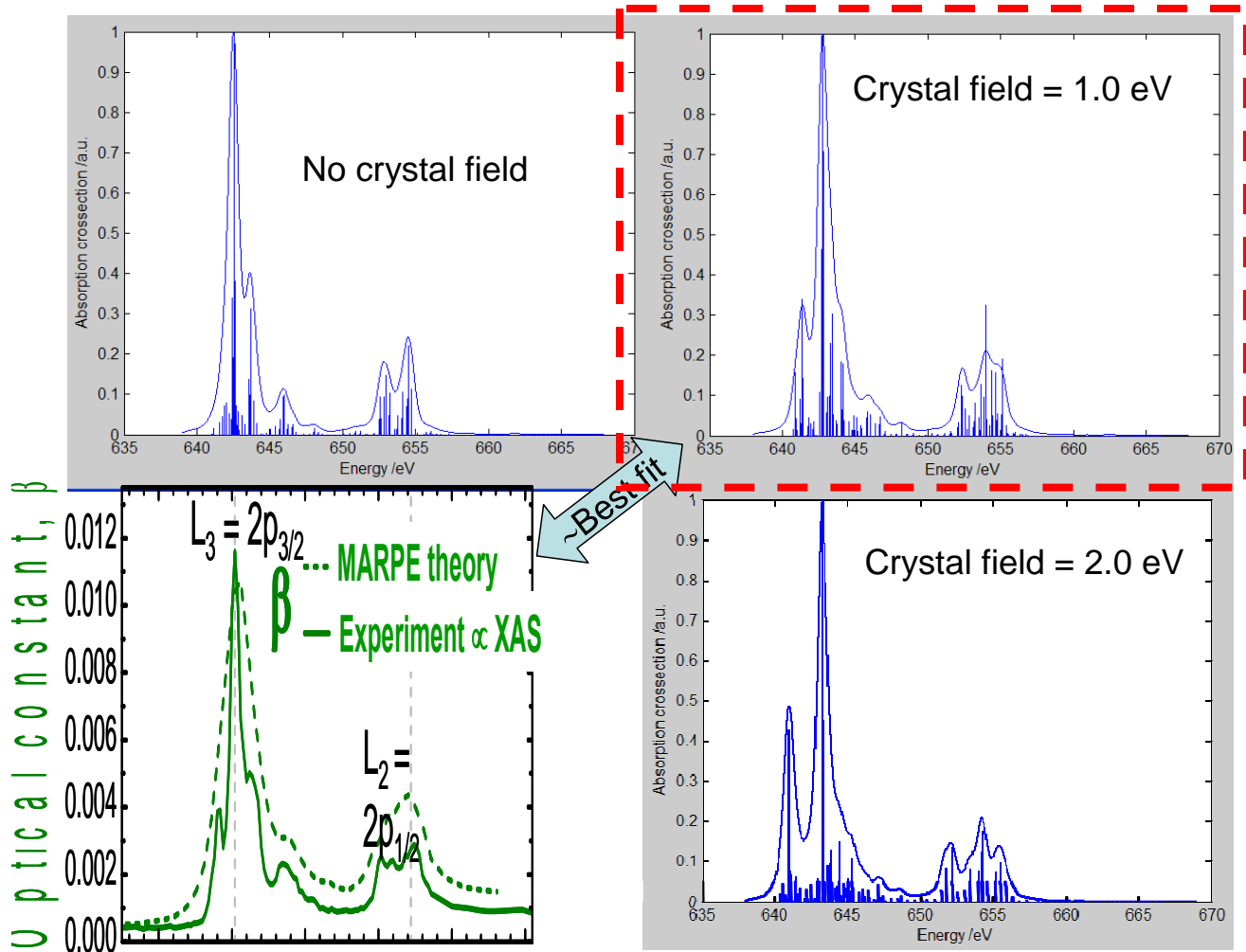
Charge transfer parameters (eV):

- Delta: T(b1)
- Udd: T(a1)
- Upd: T(b2)
- T(e)

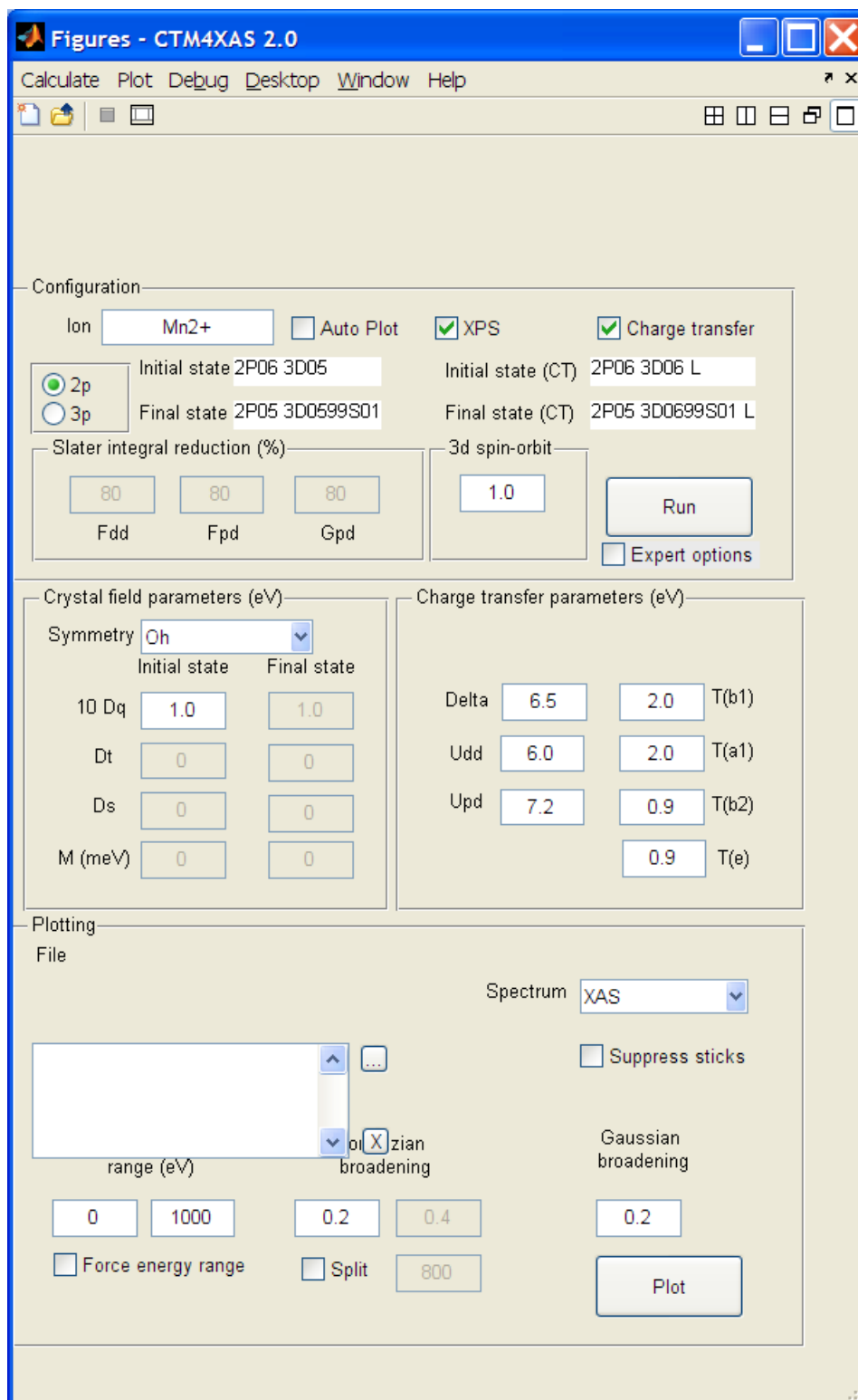
Plotting:

- File:
- Spectrum:
- Suppress sticks
- range (eV):
- Gaussian broadening:
-
- Force energy range
- Split:
-

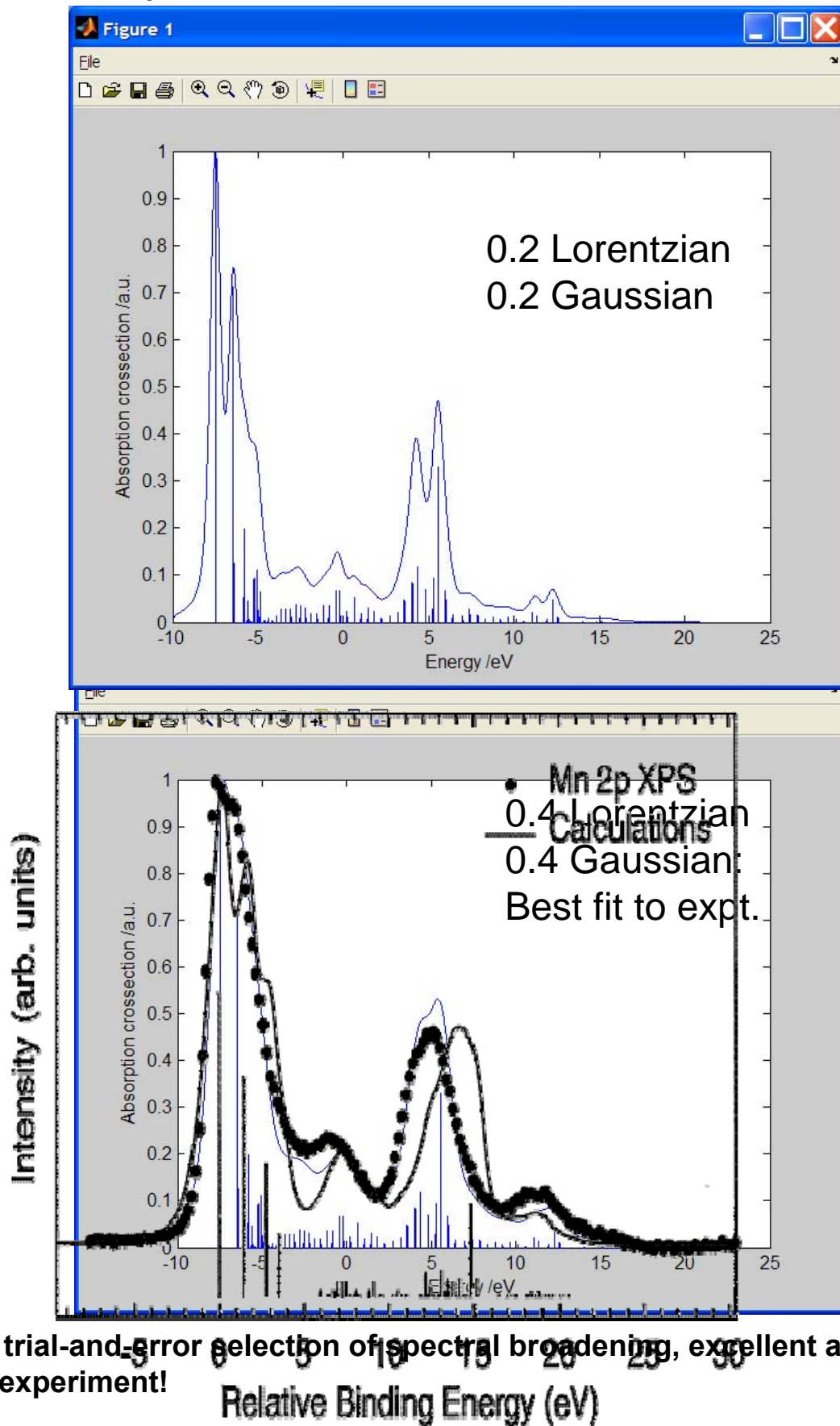
With a final result like that in our manual, where the effects of crystal field splitting were also investigated:



For XPS, the inputs look like:



And the XPS output looks like:



With trial-and-error selection of spectral broadening, excellent agreement with experiment!

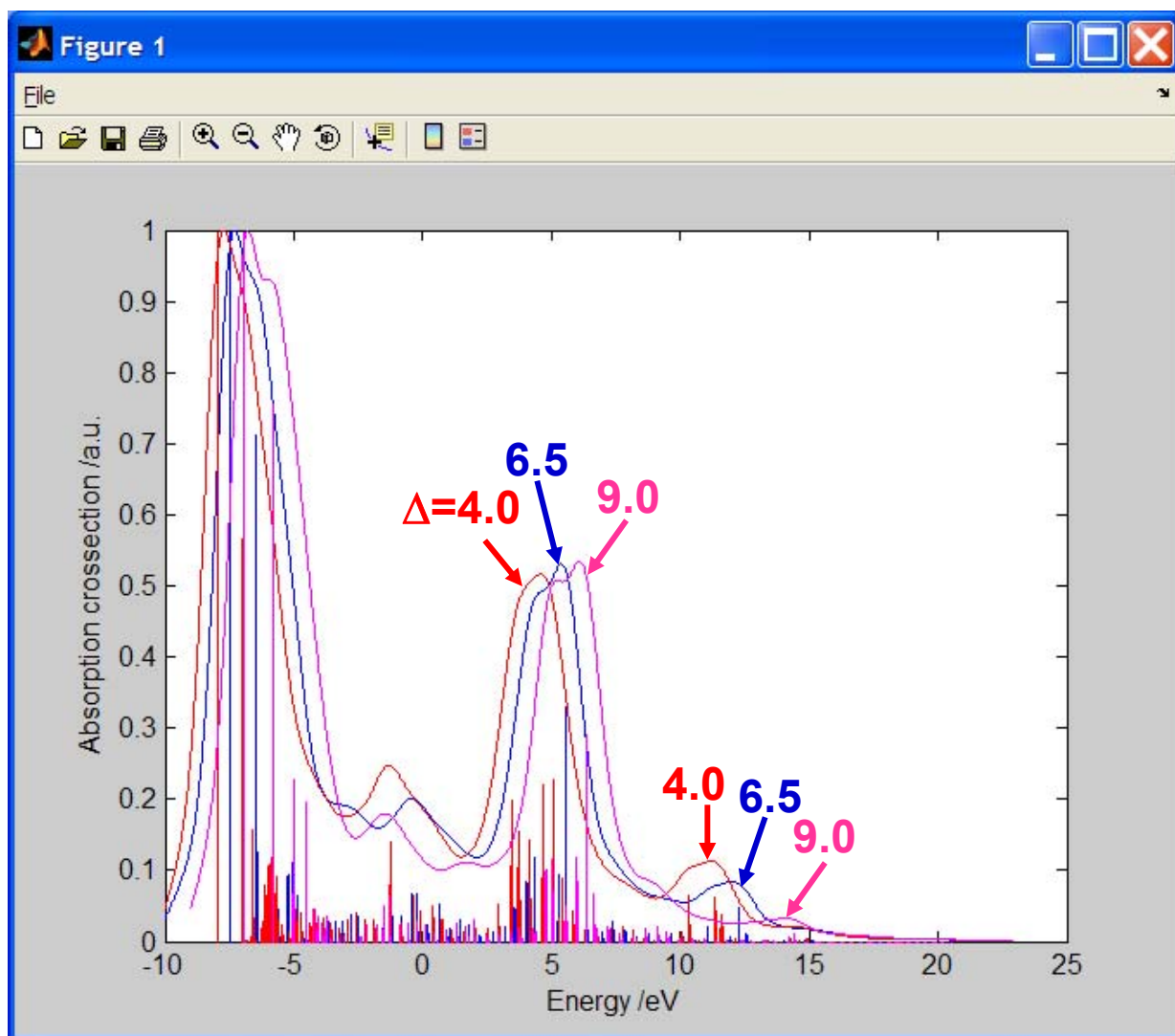
(b) Everything in this calculation is done in the Sudden Approximation limit, and with the assumption that the matrix elements for 2p excitation do not change significantly with photon energy. So you don't need to know it to do the calculation. In real life, different transitions could have different angular dependences in a single crystal for example.

(c) Can try just some extreme values around those of the optimum calculated before:

$\Delta = 4$ and 9 with 6.5 eV midway between them

$U_{dd} = 4$ and 8 with 6 midway

$U_{dp} = 5.2$ and 9.2 with 7.2 midway

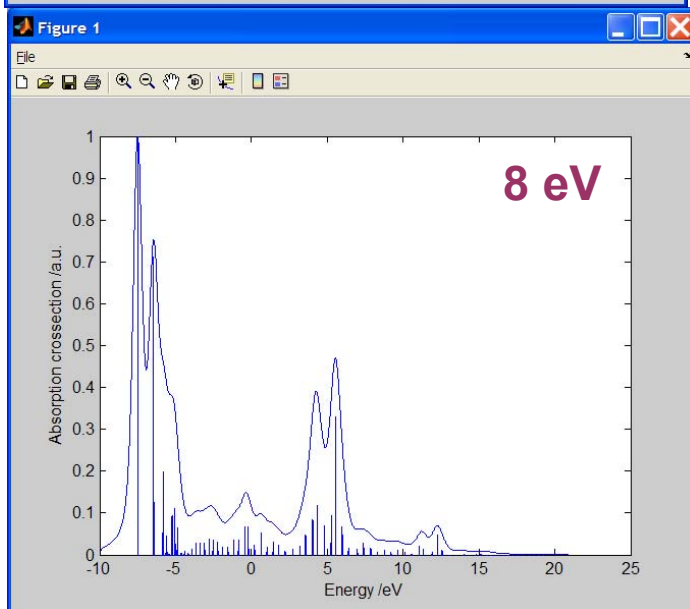
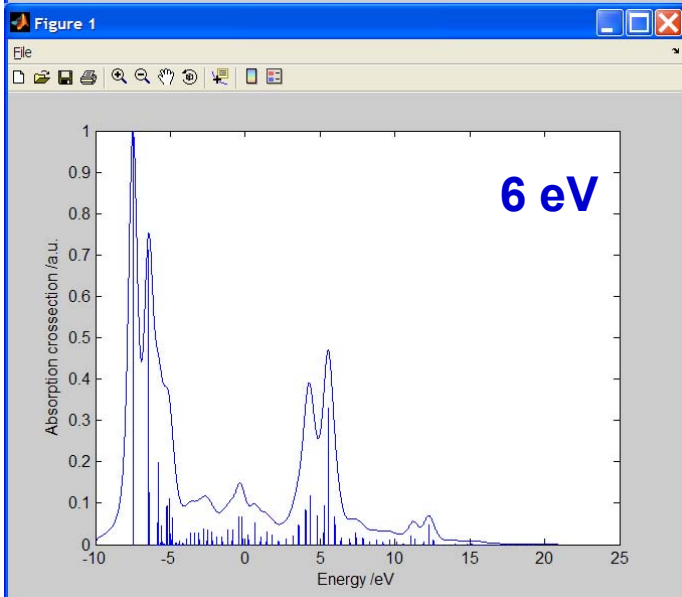
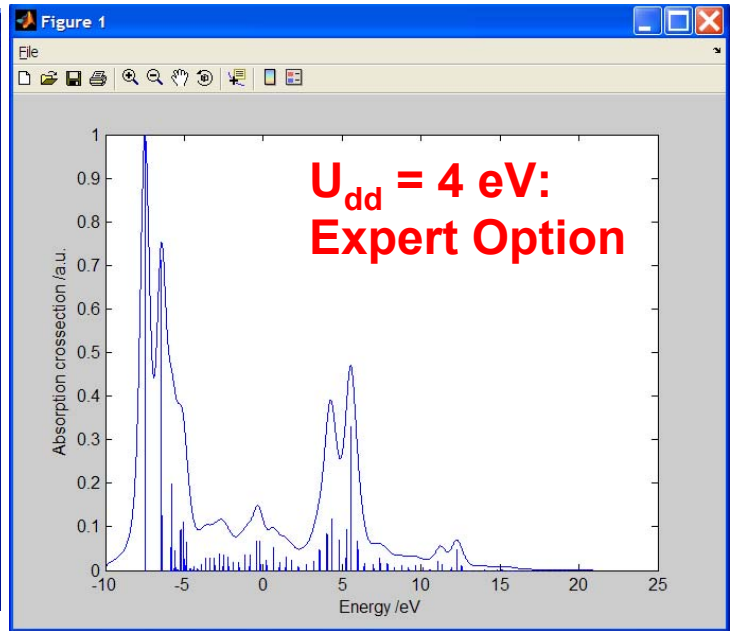
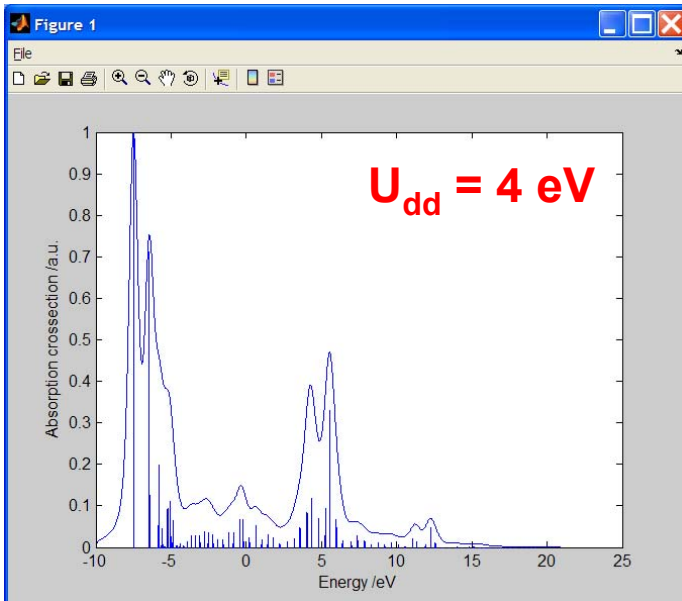


Increasing Δ with all other param. fixed decreases the unscreened satellite peak intensity, as seen also by Bocquet and Fujimori (see next page)

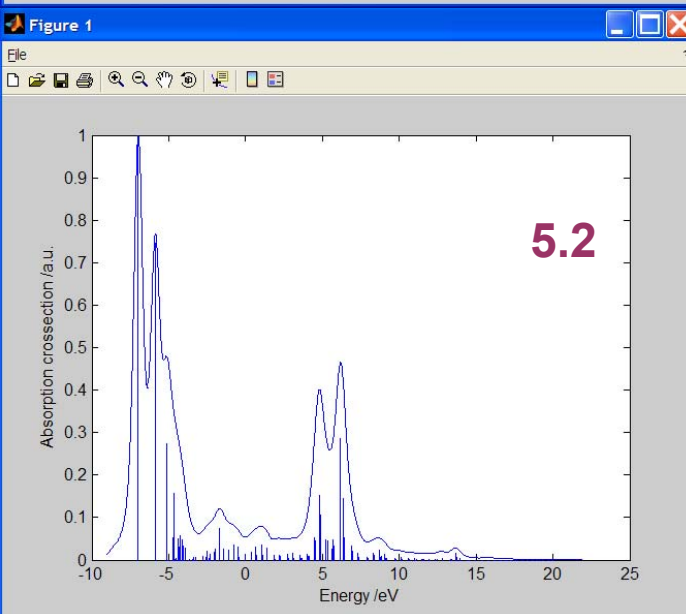
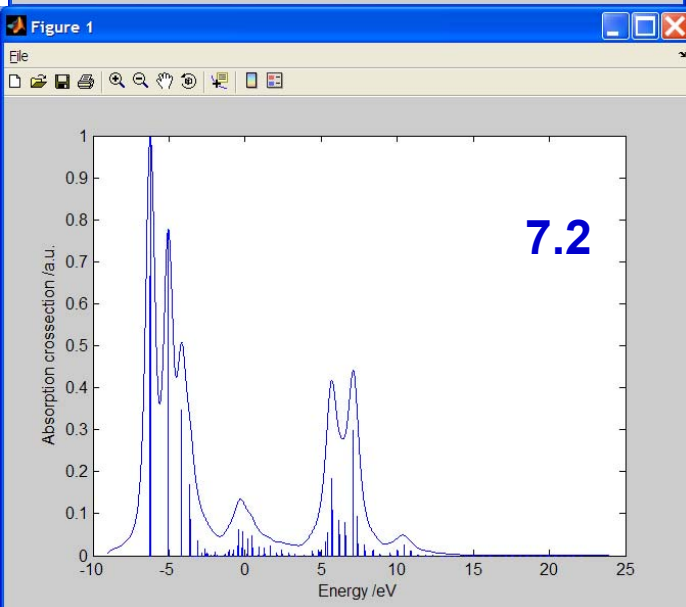
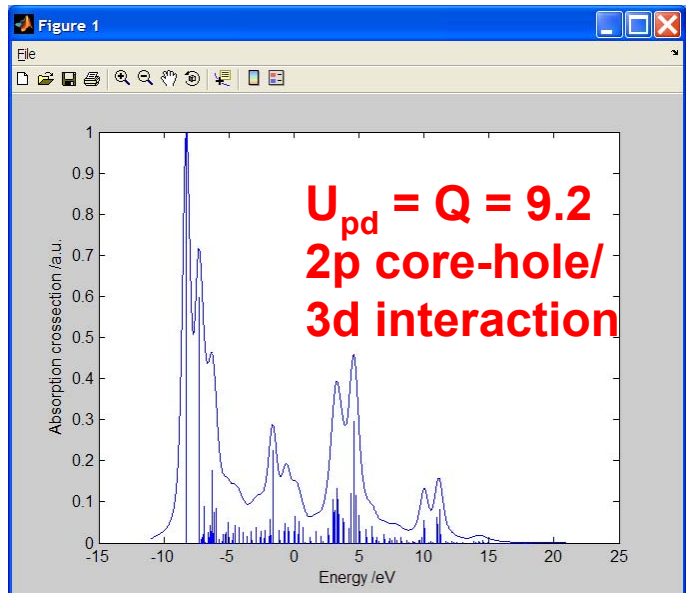
From Bocquet and Fujimori

Journal of Electron Spectroscopy and Related Phenomena 82 (1996) 87–124

General trends as Δ , U and T are varied can be observed for all TM ions studied. Where only one satellite structure is predicted, an increase in Δ leads to a fall in the satellite intensity. For $\Delta < Q$, a second (or third) satellite at higher energy may appear due to increased weight in the $cd^{n+2}\underline{L}^2$ final state (or higher final states). As Δ is increased, spectral weight from this satellite is transferred to the main satellite structure closer to the main peak, causing the main satellite first to increase and then finally to decrease as Δ approaches Q . Increasing U (and Q) with Δ and T held constant has the effect of increasing the weight of the satellite structure. As more polarizable ligands will screen the d-electrons to a greater extent, chalcogenides should be chosen with a smaller U than oxides [1]. As the hybridization strength T is increased, all satellites are found to become weaker and move away from the main peak. As T becomes larger the position and intensity of the satellite feature vary more slowly with Δ and U .



This variation didn't work: The program is obstinate in not letting one change U_{dd} , so I'm sorry about asking for this!!! Next time the program or the problem statement will be fixed.

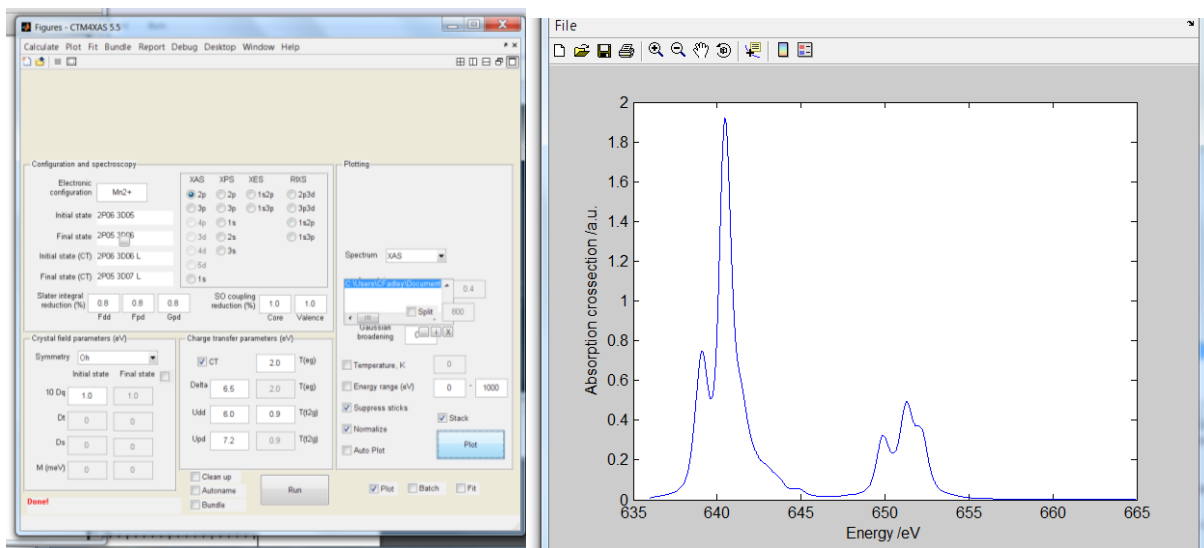


**This variation works:
As in Bocquet and
Fujimori,
Increasing U_{pd} increases
satellite intensity.
Spectrum shifts to
higher binding energy
also, as core hole drags
states down.**

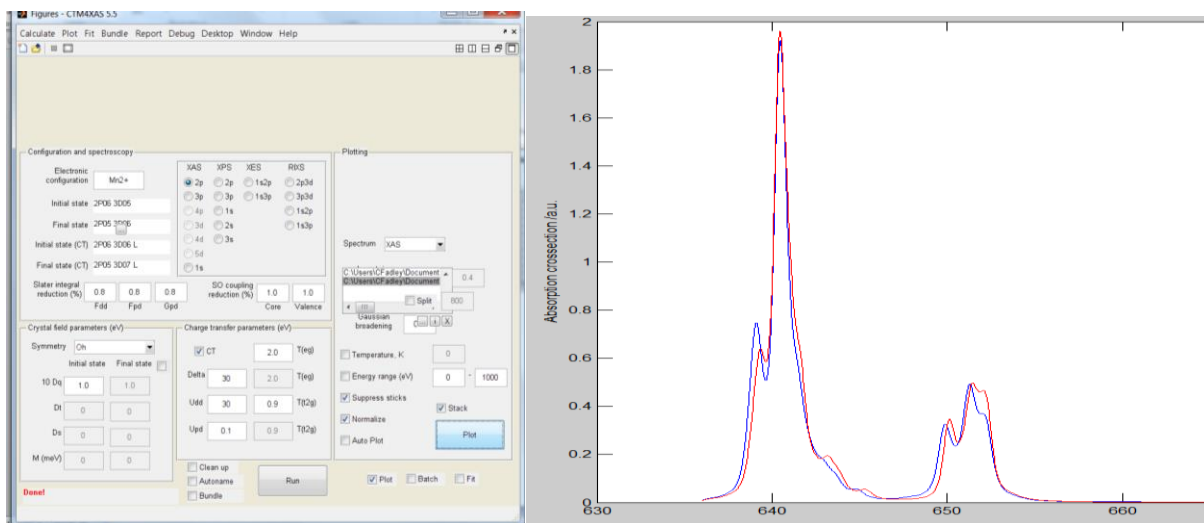
[5.10]

(d) Two calculations run with the new version of CTM4XAS5, one with charge transfer and one without, first by parameter trick of setting Δ to a very large number of 30, the core-hole attractive energy to a very small number of 0.1, and the dd repulsion to a very large number.

With charge transfer:

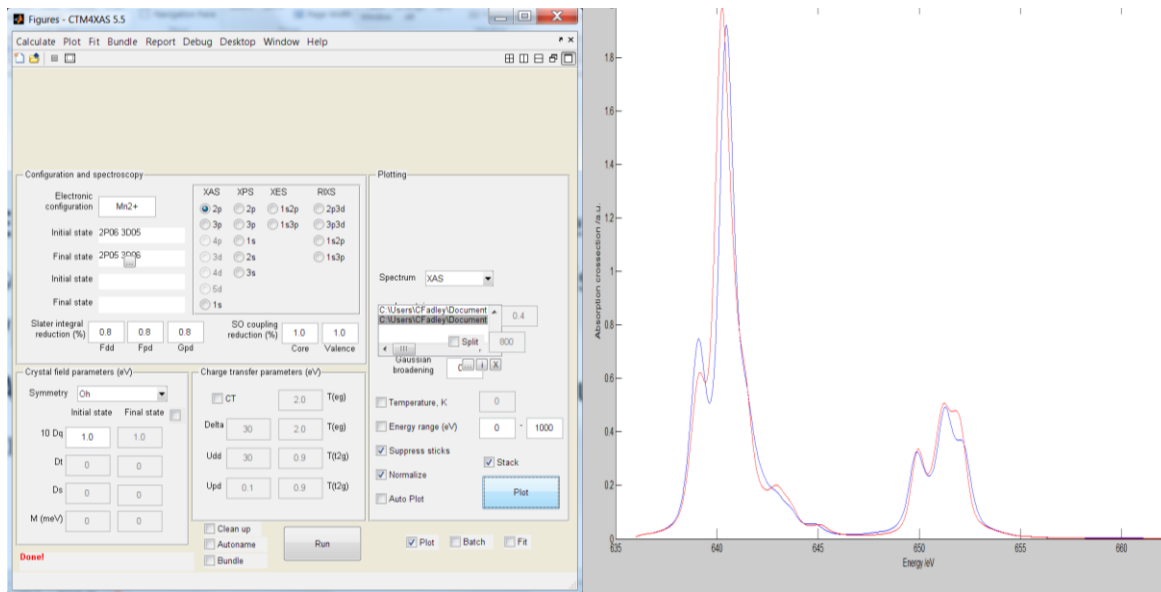


Without charge transfer using parameter trick-red curve



Effect is rather small in XAS, as the excited electron acts to screen the core hole, and the atom is in some sense left “neutral”. Slight reduction in energy of two edges with charge transfer.

Without charge transfer done simply by unclicking the charge transfer option:



Gives very nearly the same result, as expected.